

The plane with parallel coordinates

Alfred Inselberg

IBM Scientific Center,
11601 Wilshire Boulevard,
Los Angeles, CA 90025 1738, USA
Department of Computer Science
University of California
Los Angeles, CA 90024, USA

By means of *Parallel Coordinates* planar "graphs" of multivariate relations are obtained. Certain properties of the relationship correspond to the geometrical properties of its graph. On the plane a point \leftrightarrow line duality with several interesting properties is induced. A new duality between bounded and unbounded convex sets and hstars (a generalization of hyperbolas) and between Convex Unions and Intersections is found. This motivates some efficient Convexity algorithms and other results in Computational Geometry. There is also a surprising "cusp" \leftrightarrow "inflection point" duality. The narrative ends with a preview of the corresponding results in R^N .

Key words: Convexity – Duality – Parallel coordinates – Intelligent control

THE FASCINATION WITH "DIMENSIONALITY" surely predates Aristotle and Ptolemy who argued that space had *only* three dimensions.

By the nineteenth century Riemann, Lobachevsky and Gauss unshackled the imagination and with their work higher-dimensional geometries came into their own. The *perceptual experience* of higher-dimensional spaces is limited by our 3-dimensional habitation. Still it has been unsatisfying to explore properties of such *geometries* only in the abstract. From a different direction there is the motivation to obtain geometrical models (i.e. like graphs for the case of 2 or 3 variables) of multivariate relationships arising in important applications. Consequently, various methods for "visualizing" higher-dimensional spaces ([2, 3, 5, 7]) have come about aided especially by recent developments in Computer Graphics.

Here a method is proposed for obtaining geometrical models (in fact planar diagrams) of relationships in N -variables which:

1. applies for *any* positive integer N and can be extended to spaces with dimensions N_0 and N_1 ,
2. is the *same* for any N ,
3. has complexity of the representation increasing *linearly* with N and,
4. gives rise to a number of efficient geometrical algorithms.

This is accomplished by means of a mapping $R^N \rightarrow R^2$ obtained via a system of *Parallel Coordinates*, for *any positive integer* N . In this paper the fundamentals of the Parallel Coordinates for the Euclidean plane, R^2 , embedded in the

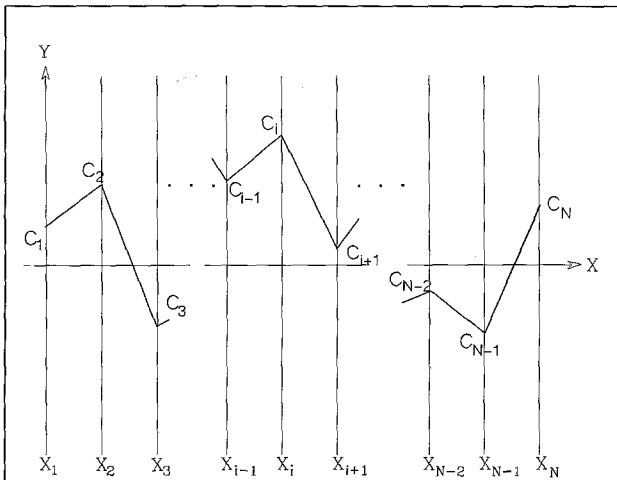


Fig. 1. Parallel axes for R^N

Projective Plane are derived, followed by a preview of some results for R^N .

Definition of parallel coordinates

For any positive integer N , a coordinate system for Euclidean N -Dimensional space R^N is constructed. On the plane with xy -Cartesian coordinates, and starting on the y -axis, N copies of the real line, labeled x_1, x_2, \dots, x_N , are placed equidistant (one unit apart) and perpendicular to the x -axis. They are the axes of the *parallel coordinate* system and all have the same positive orientation as the y -axis (see Fig. 1). A point C with coordinates (c_1, c_2, \dots, c_N) is represented by the polygonal line whose N vertices are at $(i-1, c_i)$ on the x_i -axis for $i=1, \dots, N$. In effect, a 1-1 correspondence between points in R^N and planar polygonal lines with vertices on x_1, x_2, \dots, x_N is established. Strictly speaking we consider the polygonal line representing a point as consisting not only of the *segments* between the two adjacent axes but the *whole lines containing the segments*. The need for this will become clear as the narrative develops. A *convex* hypersurface in R^N is represented in parallel coordinates by the envelope of the family of polygonal lines representing all points on the hypersurface (for an old but pleasing treatment of the theory of envelopes see [19]). Later we will need to extend the definition somewhat. The envelope, being a planar curve, is described in terms of the xy -coordinate system. Other than a superficial resemblance to nomography (see [6]) the method seems to be new. Some other methods of multivariate data representation are described in [3]. In order to:

1. Present this material in installments of manageable size,
2. Become accustomed with this representation in a relatively simple and familiar setting and
3. Contrast this coordinate system with the orthogonal coordinates,

we first study the *plane* (i.e. R^2 embedded in the Projective Plane) with parallel coordinates. The results are surprisingly rich and interesting on their own merits. Also they form the basis for the study of R^N with parallel coordinates which will be presented subsequently.

The fundamental duality

Points and lines in the plane

Points are denoted by capital and lines by lowercase letters respectively. Sets are denoted by two or more caps, while a string of caps and lowercase letters denotes a figure (i.e. a collection of lines and points). In parallel coordinates, the corresponding symbols are shown with a bar superscript (i.e. \bar{l} represents the line l , \bar{P} represents the point P etc.). Points on the plane are represented by segments between the x_1 and x_2 -axis and, in fact, by the *line* containing the segment. Consider now the x_1x_2 -plane with parallel as well as Cartesian coordinates as shown in Fig. 2 and the line:

$$l: x_2 = mx_1 + b, \quad m < \infty. \quad (1)$$

The points on l as represented in parallel coordinates form an infinite family of lines. When $m \neq 1$, any two of these lines interest at the point

$$\bar{l}: \left(\frac{1}{1-m}, \frac{b}{1-m} \right). \quad (2)$$

The distance between the parallel axes is one and the coordinates of \bar{l} are given with respect to the xy -Cartesian coordinates. It is an easy application of the theory of envelopes to show that \bar{l} is the *envelope* of the lines representing the points on the line l . Remarkably then, the

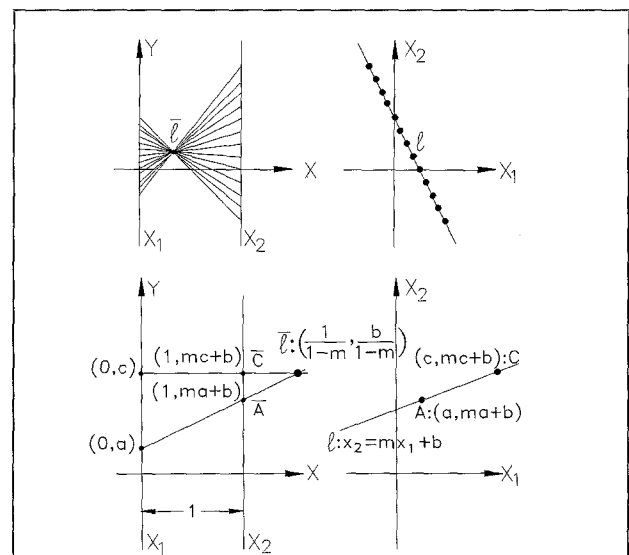


Fig. 2. In the plane parallel coordinates induce duality

line l is represented by the point \bar{l} in parallel coordinates. The correspondence for vertical lines is

$$l: x_1 = c \leftrightarrow \bar{l}: (0, c).$$

Correlation

Lines with $m=1$, as (2) suggests, do not have a corresponding point representation in the Euclidean plane. However, considering xy and x_1x_2 as two copies of the *Projective Plane* (for an elementary development of Projective Geometry see [8, 10] or [1]), the line

$$l: x_2 = x_1 + b \quad (3)$$

corresponds to the *ideal point* \bar{l} with tangent direction (i.e. slope) $y/x = b$. Conversely, in the x_1x_2 -projective plane the *ideal point* with slope m is mapped into the *vertical line* at $x = 1/(1-m)$ of the xy -projective plane. Hence, we have arrived at a *duality* between points and lines (or lines containing segments representing points) of the Projective Plane. This duality can be conveniently expressed with homogeneous coordinates as a linear non-singular transformation A – *correlation* – between the line coordinates $[m, -1, b]$ of l and the point coordinates $(1, b, 1-m)$ of \bar{l} . Specifically, the correlation

$$C_A: l \leftrightarrow \bar{l}, \quad k(\bar{l}) = A[l]$$

where $[l]$ and (\bar{l}) , the line and point (homogeneous) coordinates respectively, are taken as *column vectors*, k is a proportionality constant and

$$A = \begin{bmatrix} 0 & -1 & 0 \\ 0 & 0 & 1 \\ -1 & -1 & 0 \end{bmatrix}, \quad A^{-1} = \begin{bmatrix} 1 & 0 & -1 \\ -1 & 0 & 0 \\ 0 & 1 & 0 \end{bmatrix},$$

maps lines of the x_1x_2 -plane into *points* of the xy -plane. Dually, from $(P) = (a_1, a_2, 1)$ and $[\bar{P}] = [a_2 - a_1, -1, a_1]$ we obtain the correlation

$$C_B: P \leftrightarrow \bar{P}, \quad k[\bar{P}] = B^{-1}(P)$$

where (P) , $[\bar{P}]$ are point and line coordinates respectively and

$$B^{-1} = \begin{bmatrix} -1 & 1 & 0 \\ 0 & 0 & -1 \\ 1 & 0 & 0 \end{bmatrix}, \quad B = \begin{bmatrix} 0 & 0 & 1 \\ 1 & 0 & 1 \\ 0 & -1 & 0 \end{bmatrix},$$

maps *points* of the x_1x_2 -plane into *lines* of the xy -plane. Incidentally, inspection of the ma-

trices shows that the computation involved in going to and from parallel coordinates is fairly minimal.

Parallel lines and the ideal line

In Fig. 3 we see that \bar{l} is to the right of the x_2 -parallel axis for $0 < m(l) < 1$, on the strip between the axis for $m(l) < 0$ and to the left of the

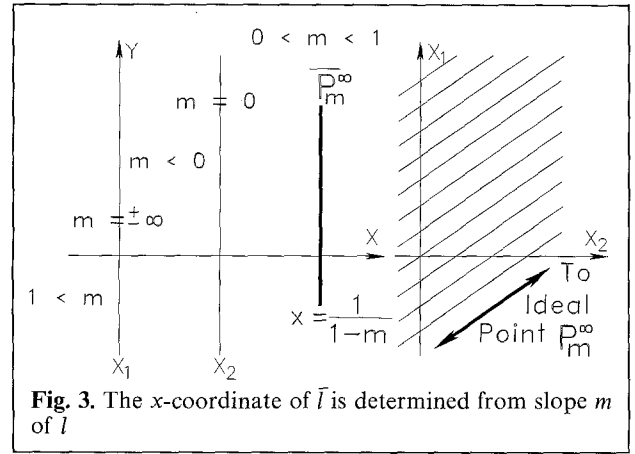


Fig. 3. The x -coordinate of \bar{l} is determined from slope m of l

x_1 -axis when $m(l) > 1$. Horizontal and vertical lines are represented by points on the x_2 -axis and x_1 -axis respectively. So another consequence of (2) is that $x(l_1) = x(\bar{l}_2) \Leftrightarrow l_1$ is parallel to l_2 . This property enables us to “eyeball” points representing parallel lines. Let us denote by P_m^∞ the *ideal point* where all lines with slope m meet. Then, our previous remark is equivalent to P_m^∞ is a vertical line in the xy -plane at $x = 1/(1-m)$ as shown in Fig. 3. Altogether then, our correlation maps the set of all lines with slope m onto the vertical line $x = 1/(1-m)$ of the xy -plane. Conversely, the set of lines with slope b in the xy -plane is mapped onto the line (3). Sets of orthogonal lines can also be represented in parallel coordinates. This is more conveniently done after some basic transformations are discussed. The collection of all ideal points of the x_1x_2 -plane is called the *ideal line* and is denoted here by l_∞ . From the *line coordinates* $[0, 0, 1]$ of l_∞ and C_A we find $(\bar{l}_\infty) = (0, 1, 0)$, an *ideal point* of the xy -plane, while from the *point coordinates* of the ideal point (P_m^∞) are $(1, m, 0)$ ¹

¹ Recall that if the homogeneous coordinates of a point P are $(P) = (a_1, a_2, a_3)$, P is an ideal point $\Leftrightarrow a_3 = 0$. Then a_1/a_2 is the slope of the parallel lines sharing (i.e. “meeting” at) this ideal point

and C_B we find $[\bar{P}_m^\infty] = [m-1, 0, 1]$, the line coordinates of $x=1/(1-m)$. Therefore, all vertical lines in the xy -plane "meet" at the ideal point \bar{l}_∞ . Reversing the argument we obtain that the ideal line \bar{L}^∞ of the xy -plane is mapped into the ideal point P_1^∞ of the x_1x_2 -plane, where all the lines with slope $m=1$ "meet".

Segments, intersections and figures

As shown in Fig. 4 for $x_1(A) < x_1(B)$ the interval $[A, B] \subset l$ in parallel coordinates looks like a "fan" i.e. the two lines \bar{A} and \bar{B} intersecting at the point \bar{l} . Then, $P \in [A, B] \Leftrightarrow x_1(P) \in I_1 = [x_1(A), x_1(B)]$ and $\bar{l} \in \bar{P}$. As well, the point $P = l_1 \cap l_2$ in parallel coordinates is represented by the segment \bar{P} , between the parallel axis, on the line joining the points l_1 and l_2 . To emphasize the aspect of duality note that the substitution of the words *point* \leftrightarrow *line* yields the correct result. Specifically, to obtain the intersection property use:

2 (Points)
Lines are on 1 (Line).
Point

Interior points of convex polygons, and in fact more general sets, can be found in parallel coordinates by means of the observation shown in Fig. 5. Let the lines l_i , $i=1, 2$, and the vertical line $v: x_1 = a$ be given. The segments \bar{P}_i , where $P_i = v \cap l_i$, are found in the way shown in Fig. 4. Consequently, a point P between l_2 and

l_1 , with $x_1(P) = a$, is represented by the segment \bar{P} on v with $x_2(P_1) \leq x_2(P) \leq x_2(P_2)$. A figure aB is mapped via the correlation to the figure $\bar{a}\bar{B}$, whose edges represent vertices of aB and conversely. A connected figure is called a *chain*² (i.e. a connected sequence of edges and vertices). The image of a (closed) polygon CP is denoted by $\bar{C}\bar{P}$ whose interior for the cases of interest will be characterized later. The polygon's boundary $\partial(CP)$ is a chain so its image $\partial(\bar{C}\bar{P})$ is directly obtained via the correlation. In the ensuing, by $x_i(A)$, $i=1, 2$, we denote the i th-coordinate of the point A , by $m(l)$ the slope of a line l , and by \bar{A} – whenever the distinction is not important – either the segment representing A or the whole line containing that segment.

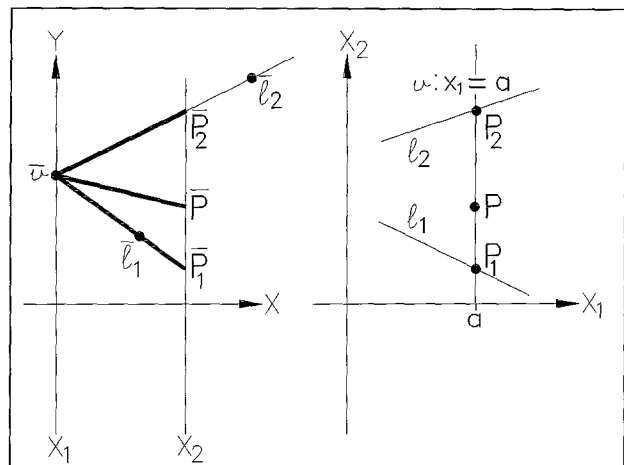


Fig. 5. Point between two lines in parallel coordinates

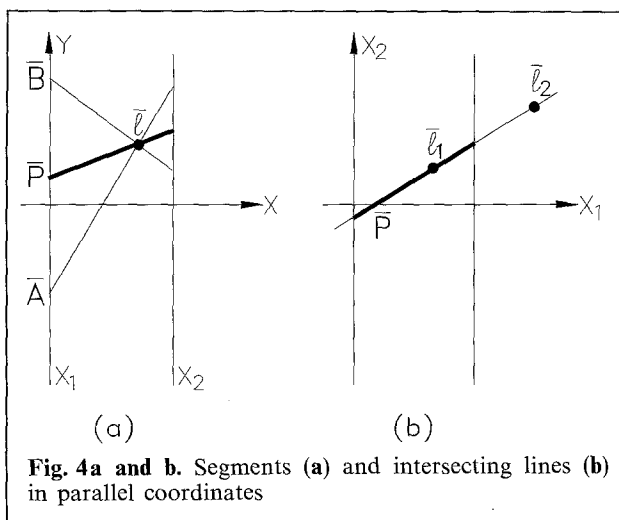


Fig. 4a and b. Segments (a) and intersecting lines (b) in parallel coordinates

A model for the projective plane

Here we describe a model of the Projective Plane to which we will appeal on occasion to aid in understanding some properties of the parallel coordinate representation. In Fig. 6 the projective plane is mapped stereographically onto a hemisphere and the disk capping it. The finite plane (consisting of "regular" points) is mapped onto the surface of the hemisphere, while each ideal point is mapped into a diameter on the disk. In fact, the coordinate system is

² Unless otherwise specified all chains considered here may have ideal points as vertices only if they are endpoints of the chain

so set-up so that the diameter's direction is the same as that of the ideal point it represents. The collection of all diameters on the cap represents the ideal line. The reader may recognize this model as a particular version of the *sphere and crosscap* classical model of the projective plane (in the spirit of those in [13] pp. 313–321). There are some advantages in looking at our correlation in terms of two copies of this model as shown in Fig. 7. A line in the x_1x_2 -plane is mapped onto a great semi-circle and the diameter corresponding to the ideal point of the line (i.e. the image of a line is a closed curve – consistent with our expectation for lines on the Projective Plane). Therefore, the images of all parallel lines “intersect” in their

common diameter (i.e. their common ideal point). In turn, each such line is mapped into a point of the xy -plane and all those points are on a vertical line mapped onto a great semi-circle and a diameter parallel to the y -axis. From our previous discussion and in terms of this model \bar{l}_∞ is mapped into the diameter parallel to the y -axis since this is the ideal point common to all P_m^∞ . Conversely, L^∞ the ideal line of the xy -plane is mapped into the ideal point P_1^∞ which is parallel to the line $x_2=x_1$ in the x_1x_2 -plane. So on the model the image of L^∞ is the diameter 45° (counter-clockwise) from the x_1 -axis.

Transformations

Let us rotate counterclockwise a line l about one of its points A . The corresponding path of \bar{l} is along the line containing the segment \bar{A} , since in any of its rotated positions l still contains the point A . Due to the counterclockwise direction of rotation the point \bar{l} moves in the direction of increasing x (i.e. to the right). In the top part of Fig. 8 a horizontal line l is rotated 180° about the origin O and the corresponding translation of the point \bar{O} along the x -axis is shown. Dually, a *translation* of a point along a line in the x_1x_2 -plane results in a *rotation* of a line about a point in the xy -plane as is illustrated in the lower part of Fig. 8.

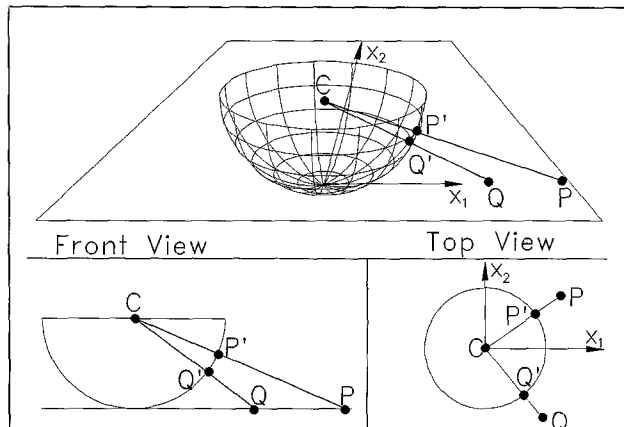


Fig. 6. A Model for the Projective Plane

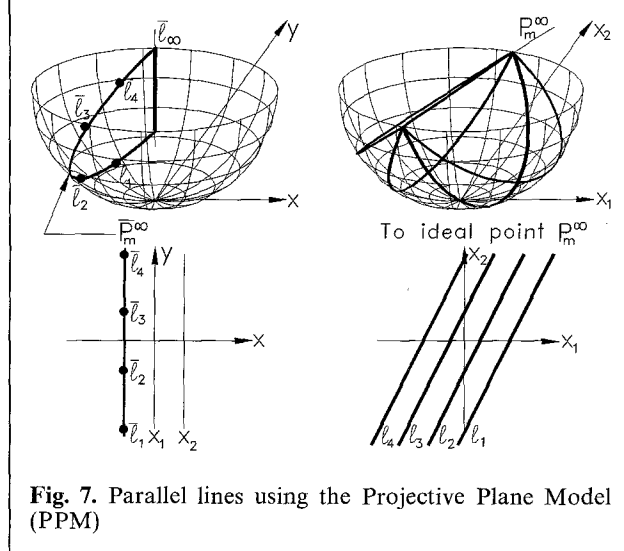


Fig. 7. Parallel lines using the Projective Plane Model (PPM)

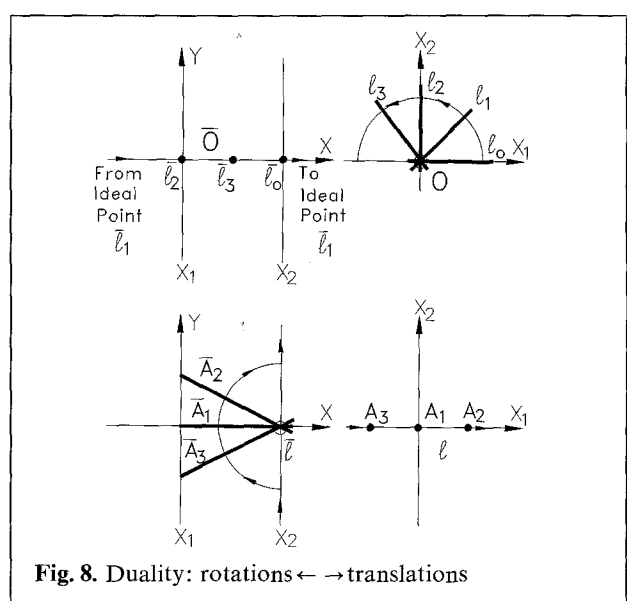


Fig. 8. Duality: rotations \leftrightarrow translations

There are two more transformations that we would like to look at next³

1. $R_{\frac{1}{2}}$, *Reflection about the line $x=\frac{1}{2}$* . In the $x-y$ -plane the reflection of the vertical line \bar{P}_m^∞ about the line $x=\frac{1}{2}$ is the line $\bar{P}_{\frac{1}{m}}^\infty$ as shown in Fig. 9.

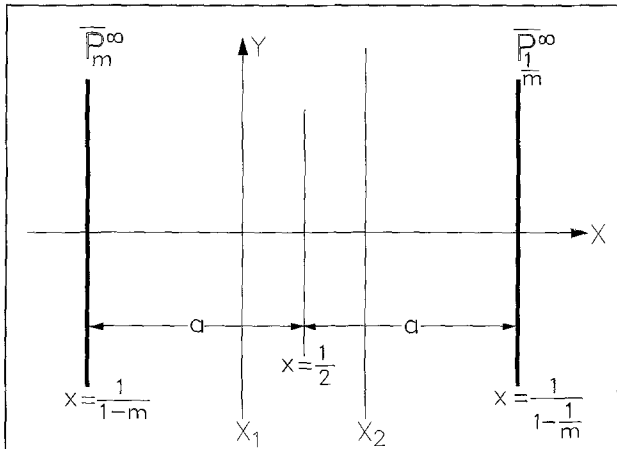


Fig. 9. Reflection about $x=1/2$

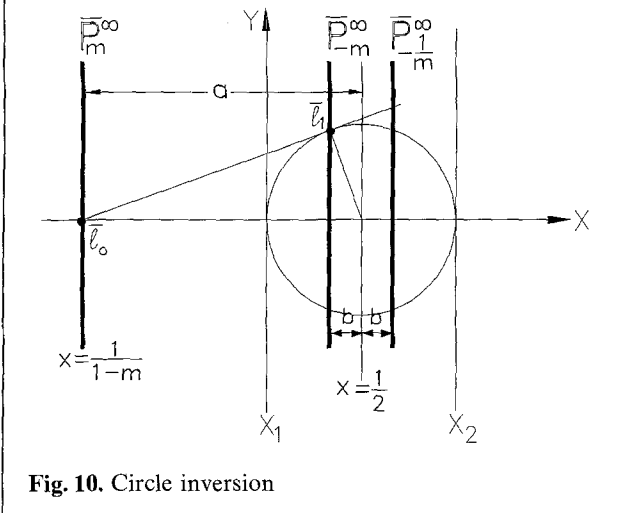


Fig. 10. Circle inversion

Therefore, such a reflection finds the image of the lines with the *reciprocal* slope – i.e. $R_{\frac{1}{2}}(\bar{P}_m) = \bar{P}_{\frac{1}{m}}$.

2. $C_{\frac{1}{2}}$, *Circle Inversion*. Consider the tangent from the point $\bar{l}_0 = \bar{P}_m \cap x\text{-axis}$ to the circle centered at $\bar{O} = (1/2, 0)$ at the point \bar{l}_1 – Fig. 10. Since $x(\bar{l}_1) = 1/(1+m)$, $C_{\frac{1}{2}}(\bar{P}_m) = \bar{P}_{-m}$.

³ I am indebted to M. Mostrel for this nice contribution

Orthogonal lines

There is an invariance pertaining to orthogonal lines. With the composition

$$R_{\frac{1}{2}} C_{\frac{1}{2}}(\bar{P}_m) = C_{\frac{1}{2}} R_{\frac{1}{2}}(\bar{P}_m) = \bar{P}_{\frac{1}{m}},$$

the image of the lines *perpendicular* to the original lines is found. Furthermore, the distances, a, b , of \bar{P}_m and \bar{P}_{-m} from \bar{O} are

$$a = -\frac{1-m}{2(1+m)}, \quad b = -\frac{1+m}{2(1-m)}$$

respectively. Therefore, $ab=1/4$ is the invariance associated between two sets of mutually orthogonal lines.

LP-Curves

Intuitively speaking, the correlation maps a *point-curve* γ into a *line-curve*, formed as the envelope of its tangents $\bar{\gamma}$. The tangent at each point of $\bar{\gamma}$ is the image – under the correlation – of the corresponding point of γ and conversely.

Definition. A set of points γ is an *LP-curve* $\Leftrightarrow \gamma = \{(x_1, x_2) | x_2 = f(x_1)\}$ where x_1 is defined on an interval (finite or infinite) of the x_1 -axis, f is a continuous function of x_1 and for each $P \in \gamma \exists a$ unique line l_p supporting γ at P .

That is, γ is a curve with a unique supporting line at each one of its points. Clearly such a curve has a well-defined representation in parallel coordinates in the sense that if γ is a line segment then $\bar{\gamma}$ is a point, else $\bar{\gamma}$ is the *envelope* of the lines \bar{P} where $P \in \gamma$. So the correlation maps the *point LP-curve* γ into the *line LP-curve* $\bar{\gamma}$ and conversely. We will consider curves which are *piecewise* (i.e. they can be partitioned into a connected sequence – a *chain* – of) *LP-curves*. A point on such a curve where two distinct *LP-curves* are joined is also called a *vertex* of the curve. An *LP-chain* $\gamma = \gamma_1 \cup \gamma_2 \cup \dots \cup \gamma_i \cup \gamma_{i+1} \cup \dots$, with $\bar{\gamma}_i$ joined to $\bar{\gamma}_{i+1}$ at \bar{V}_i (i.e. $V_i = \gamma_i \cap \gamma_{i+1}$), is mapped into $\bar{\gamma} = \bar{\gamma}_1 \cup \bar{\gamma}_2 \cup \bar{\gamma}_i \cup \bar{\gamma}_{i+1} \cup \dots$ under the correlation. At the vertex \bar{V}_i there will be two supporting lines one for each of γ_i and γ_{i+1} . In short *LP-chains* are the most general curves that have a unique parallel coordinate representation.

Let $\gamma: x_2 = f(x_1)$ be differentiable on an interval I of the x_1 -axis. The tangent to γ at the point $(x_1^0, f(x_1^0))$ is the line

$$l: x_2 = f'(x_1^0)x_1 + x_1^0 - x_1^0 f'(x_1^0).$$

Therefore, for $x_1 \in I$, $\bar{\gamma}$ is given parametrically (i.e. in terms of x_1) by:

$$\begin{aligned} x &= \frac{1}{1-f'(x_1)} \\ y &= \frac{f(x_1) - x_1 f'(x_1)}{1-f'(x_1)}. \end{aligned} \quad (4)$$

For a differentiable function $F(x_1, x_2) = 0$, $\frac{dx_2}{dx_1} = -F_{x_1}/F_{x_2}$. Hence via (4) the image $\bar{\gamma}$ of an LP-curve γ , defined by F , is given (in terms of x_1 and x_2) by:

$$\begin{aligned} x &= -\frac{\frac{\partial F}{\partial x_2}}{\left(\frac{\partial F}{\partial x_1} + \frac{\partial F}{\partial x_2}\right)} \\ y &= \frac{\left(x_1 \frac{\partial F}{\partial x_1} + x_2 \frac{\partial F}{\partial x_2}\right)}{\left(\frac{\partial F}{\partial x_1} + \frac{\partial F}{\partial x_2}\right)}. \end{aligned} \quad (5)$$

Next we show that this representation of curves is well defined.

Lemma 1. *The envelope of a function $x_2 = f(x_1)$ is unique on an interval I of the x_1 -axis where the function is differentiable.*

Proof. If two differentiable functions f_1, f_2 yield the same envelope on I then the first part of (4) yields

$$f_1(x_1) = f_2(x_1) + c_1 \quad (*)$$

for some constant c_1 , while the second part of (4) provides the condition

$$f_1' - f_2' - x_1(f_1' - f_2') + f_1'f_2' - f_2'f_1' = 0.$$

Upon substituting, $u = f_1 - f_2$, we obtain:

$$u - x_1 u' + f_2^2 \frac{d}{dx_1} \left(\frac{f_1}{f_2} \right) = 0,$$

$$\frac{u'}{u} = \frac{f_2' - 1}{f_2 - x_1} \Rightarrow f_1 = f_2(1 + c_1) - c_2 x_1. \quad (**)$$

From (*) and (**) we find that $c_1 = c_2 = 0 \Rightarrow f_1 = f_2$ q.e.d.

Convexity

Separation in the xy-plane

On the Euclidean $x_1 x_2$ -plane a point $P: (p^1, p_2)$ is on, above or below the line $l: x^2 = mx_1 + b$ if the expression $(p_2 - p_1 m)$ equals, is greater or less than b . Correspondingly, since \bar{l} is the line $y = (p_2 - p_1)m + p_1$ – see (2) – \bar{l} is on, above or below $\bar{l} \Leftrightarrow (p_2 - p_1 m)/(1-m)$ equals, is less or greater than $b/(1-m)$.⁴

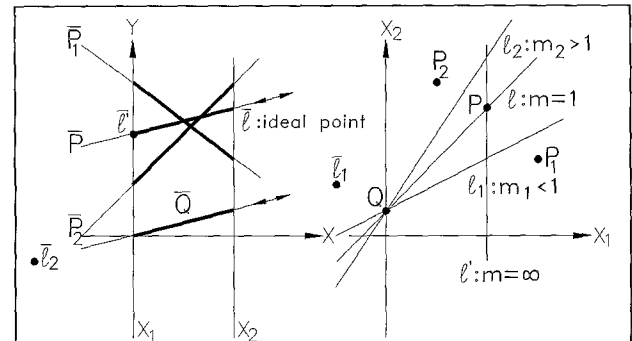


Fig. 11. Point on, above or below a line in parallel coordinates

So the comparison of $(p_2 - p_1 m)$ with b in parallel coordinates depends on whether $m < 1$ or $m > 1$ as is clearly shown in Fig. 11. Recall that l with $m=1$ induces a direction field (i.e. ideal point) with slope $\bar{m}=b$. We adopt the convention that P is on, above or below $l \Leftrightarrow \text{slope}(P)$ equals, is greater or less than $\bar{m}=b$. We consider any regular point P being below l_∞ . The various cases for $l \neq l_\infty$ are summarized in

Lemma 2. *For $m < 1$ ($m \geq 1$) l is on, below or above $P \Leftrightarrow l$ is on, below (above) or above (below) \bar{l} .*

Clearly, the image $\bar{\gamma}$ of an LP-curve γ depends on the slope of the supporting lines of γ . Denote by $l_\gamma(P)$ the unique supporting line to γ at

⁴ In general we consider a point being above (below) a segment \Leftrightarrow it is above (below) the line containing that segment

the point P , by $m_\gamma(P)$ its slope, and on an interval I of the x_1 -axis and $x_1(P) \in I$ let

$$M_\gamma(I) = \max \{m_\gamma(P) | P \in \gamma\}.$$

By considering at each vertex the supporting line with *maximum* slope, the definition of M_γ can be extended to *piecewise LP-curves*. In fact, from now unless otherwise stated all the curves considered will be *LP-chains*. As a reminder chains are allowed to have ideal points but *only as their endpoints*. There follow three direct consequences of Lemma 2 applied to *LP-chains* which are stated as lemmas. They will be useful in proving the key result of this section.

Lemma 3(a). For $M_\gamma < 1$, γ is below (above) a point $P \Leftrightarrow \bar{\gamma}$ is below (above) \bar{P} .

Lemma 3(b). For $M_\gamma \geq 1$, γ is below (above) a point $P \Leftrightarrow \bar{\gamma}$ is above (below) \bar{P} .

Proof (a). The chain γ below $P \Rightarrow \forall Q \in \gamma$ the supporting line l_Q to γ at Q is below P . Since $M_\gamma < 1$ by Lemma 2 \bar{l}_Q is below \bar{P} . Since $\bar{\gamma}$ is composed of all points which are images of supporting lines of γ , \bar{c} is below \bar{P} . The argument is reversible and the proof of (b) is entirely similar.

Lemma 4(a). γ convex downward (upward) with $M_\gamma < 1 \Rightarrow \bar{\gamma}$ is convex upward (downward).

Lemma 4(b). γ convex downward (upward) with $M_\gamma > 1 \Rightarrow \bar{\gamma}$ is convex downward (upward).

Proof (a). Any supporting line l of γ convex downward (upward) is on or below (on or above) all points $P \in \gamma$. Therefore, by Lemma 2 \bar{l} is on or below (on or above) the line $\bar{P} \Rightarrow \bar{\gamma}$ is convex upward (downward). The proof of (b) is similar.

Lemma 5. Let γ_1, γ_2 be *LP-chains* and $\gamma = \gamma_2 \cup \gamma_1$ chain⁵, then γ_1 convex upward (downward) with $M_1 < 1$ and γ_2 convex downward (upward) $M_2 \geq 1$ (i.e. γ convex downward (upward)) $\Leftrightarrow \bar{\gamma}$ convex upward (downward).

Proof. By Lemma 4 $\bar{\gamma}_1$ is convex downward (upward) and $\bar{\gamma}_2$ is convex downward (upward).

⁵ That is, if l is a supporting line of γ then all of γ is on one side (on or above, on or below) of l . Here M_i denotes the M of γ_i

Let $V = \gamma_1 \cap \gamma_2$ and l_i the supporting line to γ_i at V . Then γ_1 is on or above (on or below) its supporting line \bar{V} at \bar{V} . The same is true for γ_2 . Hence $\bar{\gamma}$ is convex upward (downward). The steps in the argument can be reversed in the proof of the converse.

Generalized conics

Specialized results on convexity have been reported elsewhere (see [16]). In order to make this narrative reasonably self contained, only the theorems on convexity with more general interest are included here. The proofs are usually different (and hopefully easier) than those given earlier. First a definition is given which is central to many of the results. It is best understood by referring to Fig. 12.

Definition 1. A set HP is *hstar* \Leftrightarrow its boundary is a closed piecewise *LP-curve* $\exists \partial(HP) = Cc_1 \cup Cc_2 \cup \{l_1, l_2\}$ Cc_1, Cc_2 are convex upward and convex downward piecewise *LP-curves* with left and right endpoints L_i, R^i respectively for $i=1, 2$, $l_j = L^j R_k$, $j \neq k$, the curves have no vertical edges, no vertical lines separates them, $l_1 \cap l_2 = W$ a regular point called the *waist*, W is below Cc_1 and above Cc_2 respectively. Finally, it is required that $\{Cc_1 \cup Cc_2\} \cap \{l_1 \cup l_2\} = \{L_1, L_2, R_1, R_2\}$. Cc_1 and Cc_2 are called the *upper* and *lower* chains, respectively of the hstar and l_1, l_2 its *asymptotes*. Note that $W \notin HP$ unless $W = Cc_1$, or

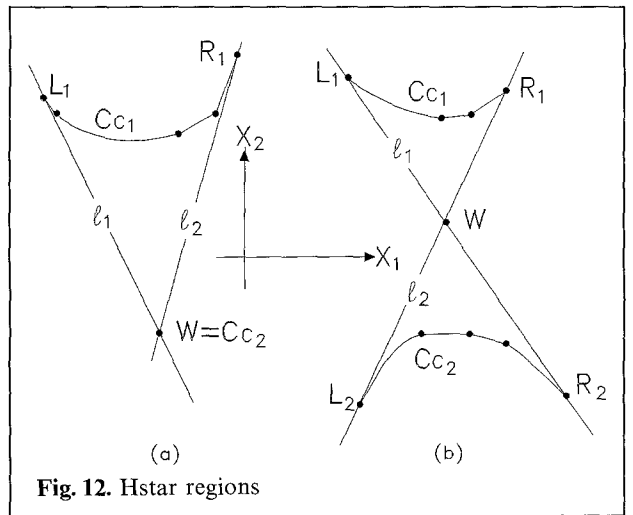


Fig. 12. Hstar regions

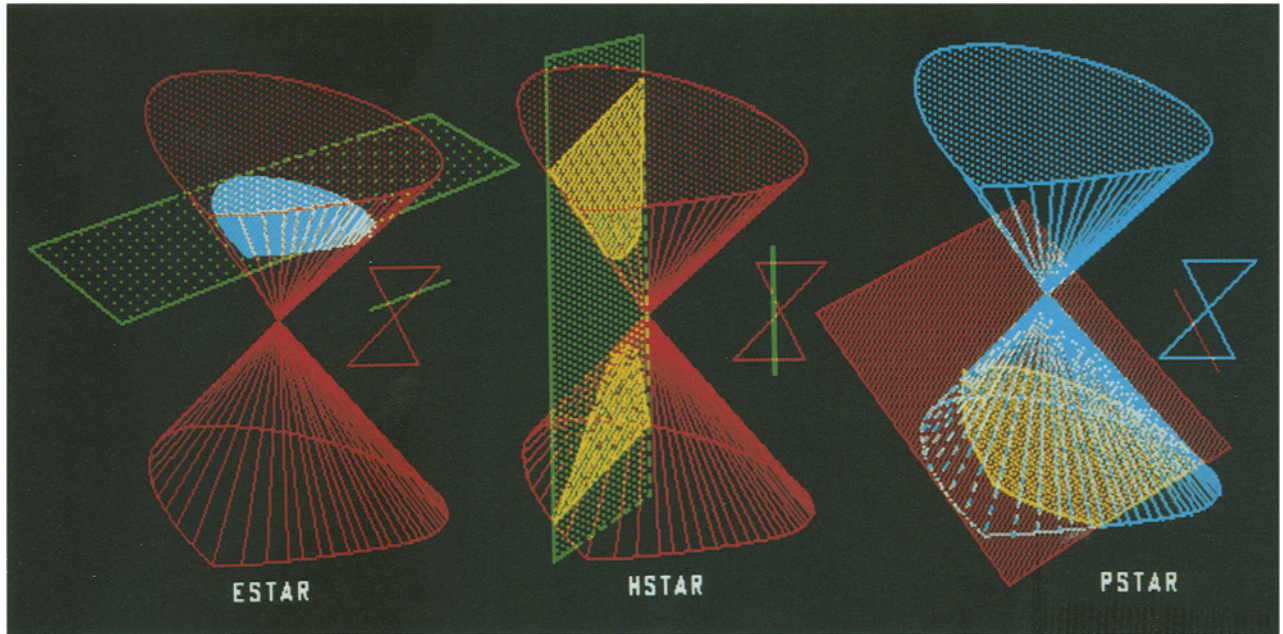


Fig. 13. Gconics

Cc_2 in which case the hstar is called *dstar* (see (a) in Fig. 12).

The term *hstar* is used here because these sets are star-regions and they resemble hyperbolas. For hstars ideal endpoints must be the same on each asymptote. That is if L_1 is an ideal point so is R_2 and $L_1=R_2$. Or, if L_2 is ideal then $L_2=R_1$. In this case there is a range of possible lines for the asymptotes. The *waist* is rendered unique by choosing among these the line having the largest possible intercept for the asymptote with the minimum slope, and the one having the smallest possible intercept for the asymptote having the maximum slope. With that choice $W=l_1 \cap l_2$. Note that for dstars a chain may consist of a single point distinct from W .⁶

Definition 2. A set HM is *hstar with respect to an ideal point having slope m* (we will use the contraction *hstar wrt to m*) \Leftrightarrow HM is hstar when the plane is rotated counterclockwise about the origin so that the lines with slope m become vertical. We refer to the upper and lower chains of CP as those which are the upper and lower chains of the rotated hstar wrt $m = \pm\infty$. As

well, the left and right endpoints of the chains in the rotated positions are also called the left and right endpoints of the respective chains.

For an hstar wrt m there are no lines with slope m that separate its two chains and its asymptotes l_i are such that $m(l_i) \neq m$. The term *hstar* by itself refers to an hstar with respect to slope $\pm\infty$.

Let CP be a closed and bounded convex set. With CP as a base let us construct a double cone as shown in Fig. 13 (for the purposes of this discussion it is immaterial whether it is a right cone or not). A plane intersecting the cone in two disjoint parts forms an *hstar*. Extending the analogy, there are two other kinds of planar sections with the cone those forming *bounded* and those resulting in *unbounded* planar (convex) sets. The bounded ones are called *estars* (the “e” for the analogy to ellipses) while the *unbounded* ones are called *pstars* (the “p” refers to their resemblance to parabolas). *Estars*, *pstars* and *hstars* are generalizations of the ordinary conics and collectively are referred to as *gconics* (see Fig. 13). Below we will see that the set of gconics is *closed* under our correlation.

Every bounded set whose boundary is an *LP*-chain has 2 distinct *bounding supporting lines* with slope some given m . In Fig. 14 this is

⁶ The reader interested in a discussion and examples of the conventions adopted for the special cases is referred to [16].

shown for an estar CP . There the bounding supporting lines v_L, v_R with slope $m = \pm\infty$ are incident at the vertices V_L and V_R where $x_1(V_L) < x_1(V_R)$ respectively. The upper and lower bounding supporting lines with slope $m=1$, CP is on or below the “upper” supporting line denoted by l_u and on or above the “lower” one denoted by l_l , are incident at the vertices V_u and V_l respectively.

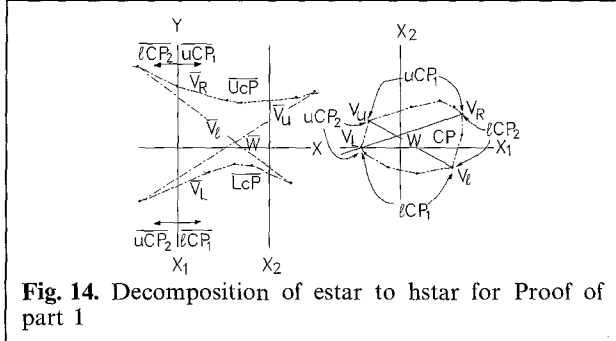


Fig. 14. Decomposition of estar to hstar for Proof of part 1

Theorem 1. CP is a gconic $\Leftrightarrow \overline{CP}$ is a gconic.

In particular,

1. CP is an estar $\Leftrightarrow \overline{CP}$ is an hstar.
2. CP is a pstar \Leftrightarrow all vertical lines intersect \overline{CP} in only one point. There are two cases:
 - a) all lines with $m=1$ intersect CP at only one point $\Leftrightarrow \overline{CP}$ is pstar, or
 - b) \exists a line with $m=1$ intersecting CP in two distinct points $\Leftrightarrow \overline{CP}$ is an hstar having one vertical asymptote.
3. CP is an hstar $\Leftrightarrow \exists$ a vertical line having no common points with \overline{CP} . There are three cases:
 - a) CP is an hstar wrt $m=1 \Leftrightarrow \overline{CP}$ is an estar,
 - b) CP is an hstar having an asymptote with slope $m=1 \Leftrightarrow \overline{CP}$ is a pstar and \exists a vertical line intersecting \overline{CP} at two distinct points, or
 - c) CP is an hstar wrt $m \neq 1$ ⁷ $\Leftrightarrow \overline{CP}$ is an hstar and \exists a vertical line separating its chains.

Proof 1. If CP is a finite segment with endpoints A, B of a line l the \overline{CP} consists of the two lines \bar{V}_u and \bar{V}_l . With our convention this is true even if $m(l)=1$. This is an hstar with waist \bar{l} and asymptotes \bar{V}_u and \bar{V}_l and empty upper and lower chains. Hence, no lines (including verticals) can separate the two chains. Otherwise, the four points V_u, V_l, V_R, V_L partition $\partial(\overline{CP})$ into four chains (see Fig. 14) uCP_i, lCP_i i

⁷ So \exists a line with $m=1$ intersecting each of CP 's chains in two distinct points

=1, 2 where $i=1$ specifies the sub-chains whose LP -arcs have supporting lines with $-\infty \leq \text{slope} < 1$ and $i=2$ those with $+\infty \geq \text{slope} \geq 1$. Let

$$\overline{UcP} = \overline{uCP_1} \cup \overline{lCP_2},$$

$$\overline{LcP} = \overline{lCP_1} \cup \overline{uCP_2}.$$

By Lemma 5 the chains \overline{UcP} and \overline{LcP} are, respectively, convex downward and convex upward. These two chains are joined by \bar{V}_l and \bar{V}_u , intersecting at \bar{w} , since $\partial(\overline{CP})$ is simply connected. Note that uCP is above and lCP is below both \bar{V}_l and \bar{V}_u respectively. So V_l, V_u are supporting lines of the chains and incident at their endpoints with \bar{w} in between the chains. We see that w splits CP into UcP and LcP . For $m(w) < 1$ UcP is above and LcP is below respectively of w , and the sides reverse when $m(w) > 1$. Of course, when $m(w)=1$, $CP=w$. To complete the proof note that by the convexity of \overline{CP} , P is an interior point of $CP \Leftrightarrow P$ is below uCP and above lCP , (via Lemma 2) $\Leftrightarrow \bar{P}$ is below uCP_1, lCP_2 (i.e. UcP) and \bar{P} is above LcP . We have proved that P is an interior point of $CP \Leftrightarrow \bar{P}$ separates LcP from UcP (see Fig. 22).⁸ Clearly no vertical line V can separate LcP from UcP for that would imply that the bounded set CP contains an ideal point V . Hence \overline{CP} is an hstar (wrt $m = \pm\infty$). To prove sufficiency we reverse the order of the decomposition shown above. Let UCp, LCp denote the upper and lower chains respectively of the hstar \overline{CP} and the subscripts 1, 2 designate the subchains whose tangents have slope \leq or > 1 respectively. That is UCp_1, LCp_1 are the subchains on or to the left of the x_1 -axis, while those to its right carry the subscript 2. Further, we denote by \bar{U}, \bar{L} the supporting lines connecting $\overline{UCp_1}$ to LCp_2 and $\overline{UCp_2}$ to LCp_1 respectively with $\bar{w} = \bar{U}\bar{L}$. Define

$$\overline{ucP} = \overline{UCp_1} \cup \overline{LCp_2} \cup \{\bar{U}\},$$

$$\overline{lcP} = \overline{UCp_2} \cup \overline{LCp_1} \cup \{\bar{L}\}.$$

It is a direct consequence of Lemma 5 that w partitions CP into the convex downward and convex upward chains ucP and lcP respectively and therefore CP is convex. The boundedness of CP follows, as above, from the nonexistence

⁸ Due to its importance, this result is also stated separately as a Corollary

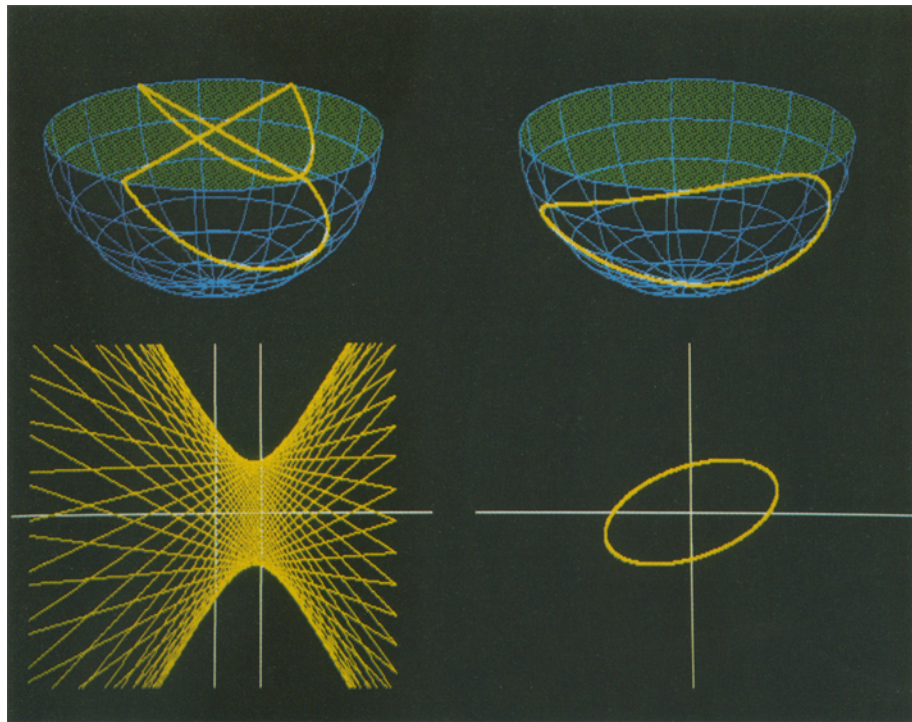


Fig. 15

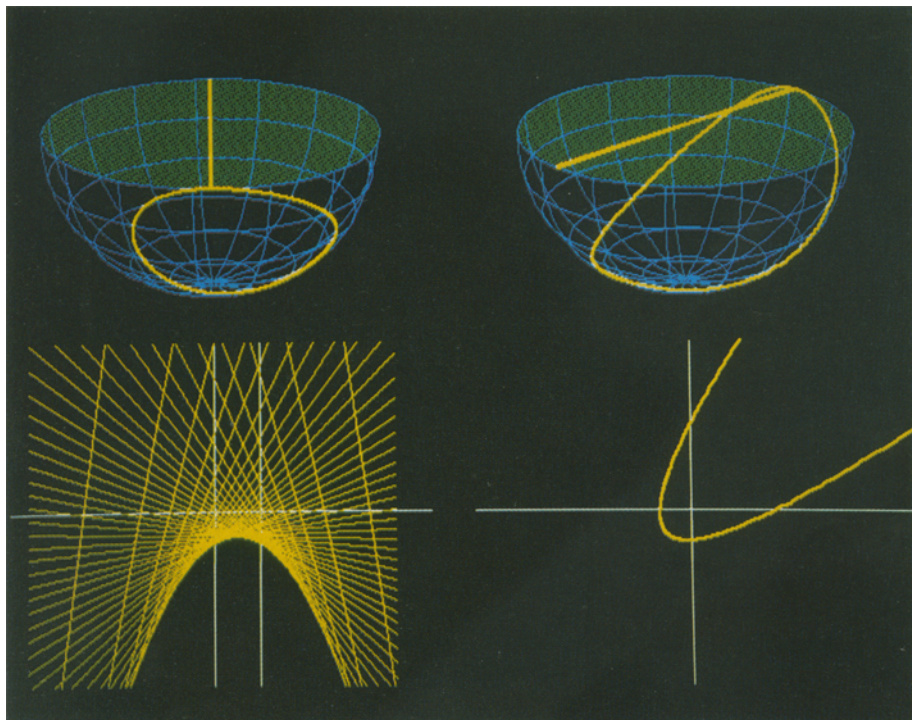


Fig. 16

Fig. 15. Part 1 of Theorem: estar to hstar, dual of 3(a)

Fig. 16. Part (2a) of Theorem: pstar to pstar, dual of 3(b)

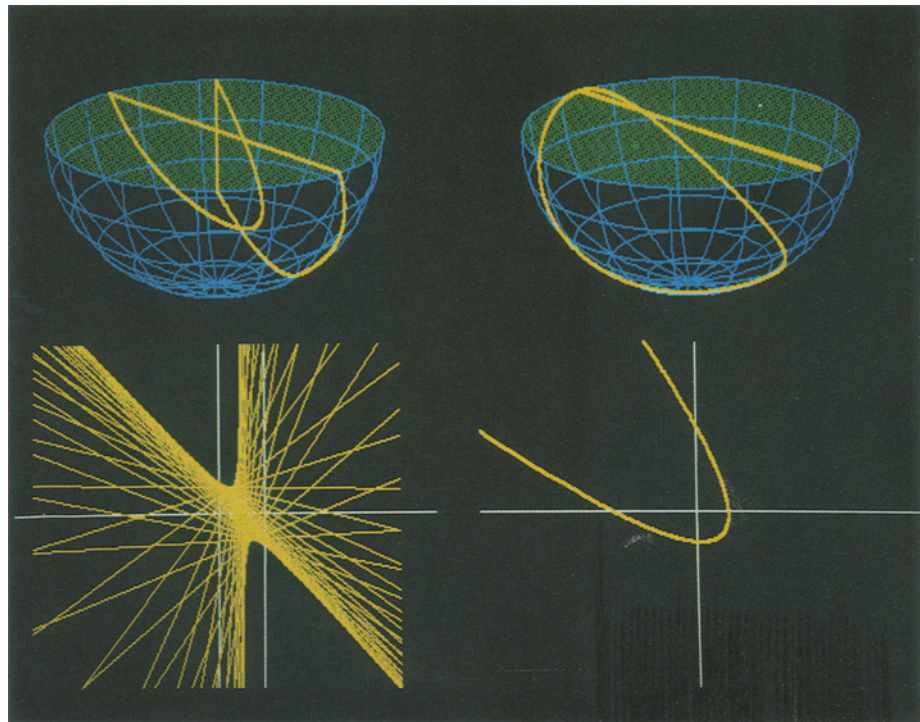


Fig. 17

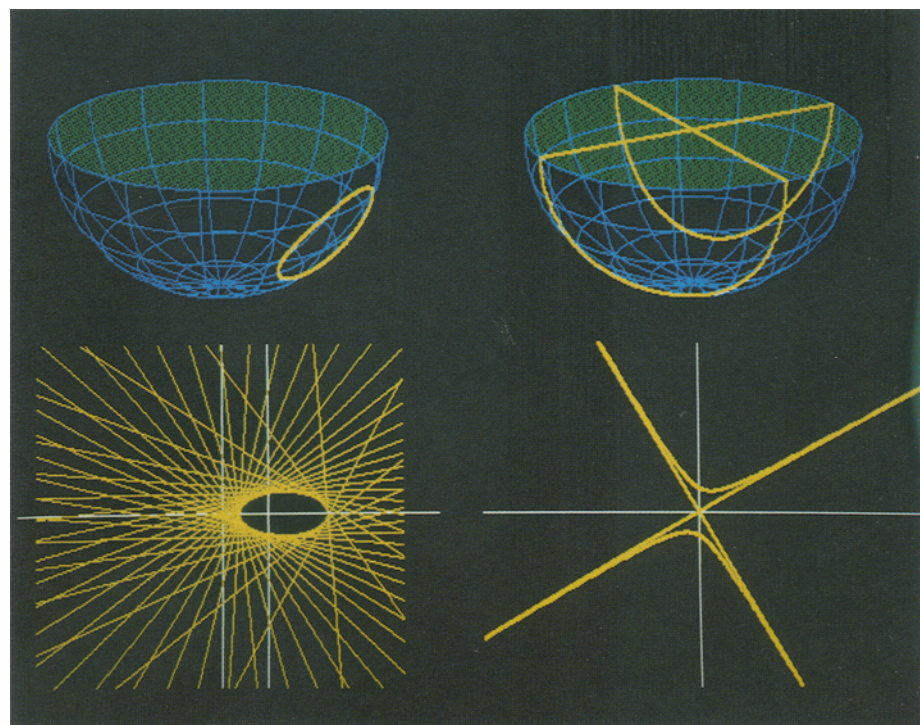


Fig. 18

Fig. 17. Part 2(b) of Theorem: pstar to hstar, self dual

Fig. 18. Part 3(a) of Theorem: hstar to estar, dual of 1(a)

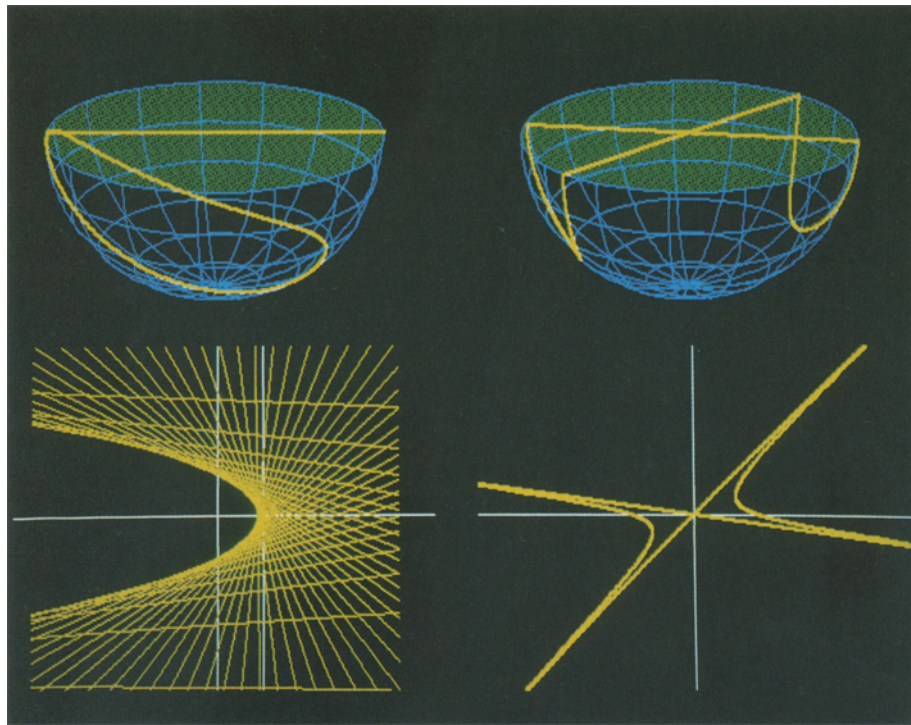


Fig. 19

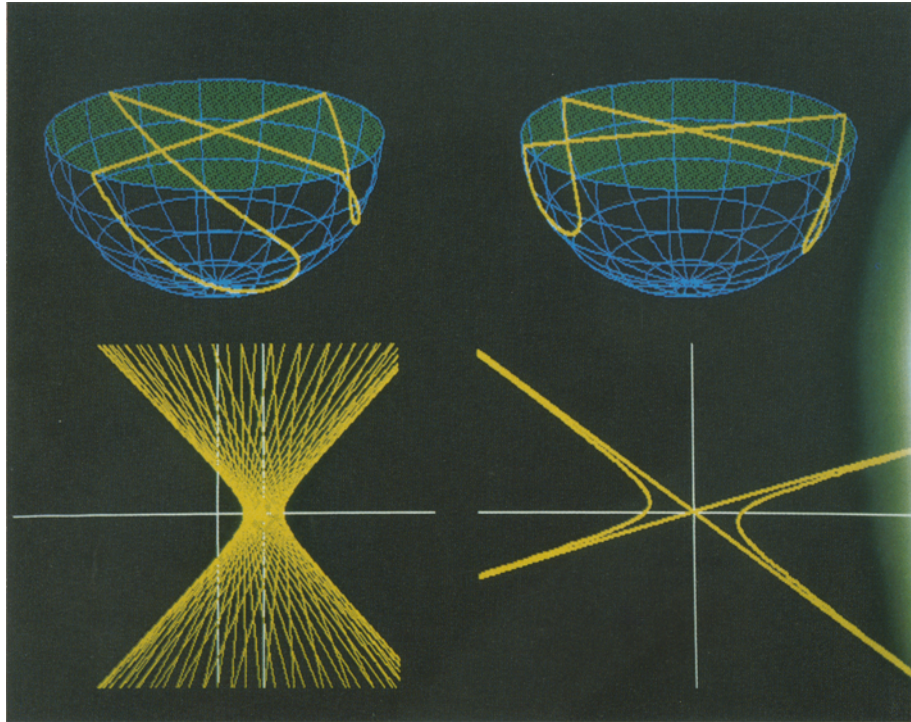


Fig. 20

Fig. 19. Part 3(b): hstar to pstar, dual of 2(b)

Fig. 20. Part 3(c): hstar to hstar, self-dual

of a vertical separatrix for \overline{ucP} , and \overline{lcP} (see also Fig. 15) q.e.d.

Proof 2(a). Here $\partial(CP)$ is convex downward (or convex upward) and is the union of two LP-chains say $\gamma_1 \cup \gamma_2$ with $M_1 < 1$ and $M_2 > 1$. Directly then by Lemma 5 \overline{CP} is convex upward (or convex downward) and unbounded, therefore it is a pstar. Since Lemma 5 is valid in both directions the converse is also true (see Fig. 16). Note that CP has no asymptotes since CP has no bounding supporting lines with $m=1$.

Proof 2(b). This is obtained directly from part 1 by allowing either V_u or V_l to be an ideal point and therefore l_∞ is one of the bounding supporting lines. In turn ideal points are mapped into the vertical asymptote of the hstar CP , while the regular point gives the nonvertical asymptote (see Fig. 17) and conversely. This case is self-dual.

Proof 3(a). This is simply the dual of 1(a) since lines with $m=1$ in the x_1x_2 -plane map into ideal points of the xy -plane and conversely. In short lines between the upper and lower chains

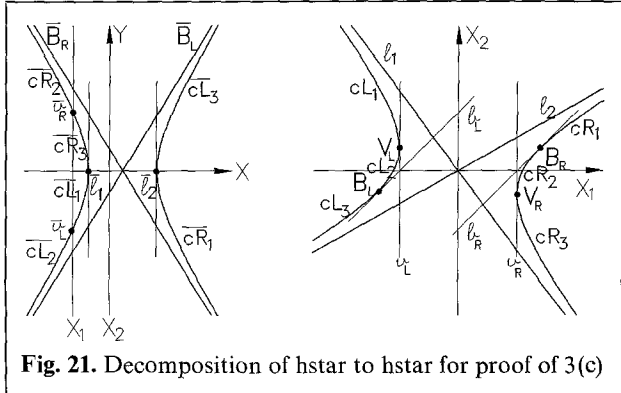


Fig. 21. Decomposition of hstar to hstar for proof of 3(c)

of the hstar map into interior points of the estar.

Proof 3(b). This is the dual of 2(b) for the same reason (see Fig. 19).

Proof 3(c). Let CP be such an hstar with asymptotes l_1, l_2 and $m(l_1) < m(l_2)$. Recall that the “upper” and “lower” chains of an hstar CP wrt m are those which after rotation of CP are the upper and lower chains respectively of the rotated hstar wrt $m = \pm\infty$. As shown in Fig. 21, for CP the chain appearing on the left (and for which the subscript L is used) corresponds to the lower and the right chain (with subscript R) corresponds to the upper one. Since \exists a line $m=1$ separating the two chains, there exist bounding lines b_L and b_R with $m=1$ of the lower chain at the point B_L and the upper chain the point B_R respectively. There also \exists supporting lines v_L, v_R with $m=\pm\infty$ of the lower and upper chains of CP at the points V_L and V_R respectively. The points $B_i, V_i, i=L, R$, divide each of the respective chains in three parts. Specifically, the lower chain is divided in the chains cL_1, cL_2, cL_3 where the odd subscripts 1 and 3 denote chains γ with $M_\gamma \leq 1$, while the subscript 2 denotes chains γ with $M_\gamma \geq 1$ and similarly for the upper chain. Note that $cL_1 \cap cL_2 = V_L$ and $cL_2 \cap cL_3 = B_L$, while $cR_1 \cap cR_2 = B_R$ and $cR_2 \cap cR_3 = V_R$.

In the first four columns of the Table 1 above the properties of the six subchains are listed. Column six is obtained via Lemma 4, and columns seven and eight are obtained from Lemma 3 and where properties of the corresponding images are listed.

To “piece” the information together in order to obtain \overline{CP} we note that $\overline{v_R}, \overline{v_L} \in x_2$ -axis,

Table 1

Curve, subs 2 for $M \geq 1$ 1, 3 for $M \leq 1$	Convex up (u) or down (d)	Above (a) or below (b) points		Image of Curve	Convex up (u) or down (d)	Above (a) or below (b) lines	
		B_R	B_L			$\overline{B_R}$	$\overline{B_L}$
cL_1	d	b	a	$\overline{cL_1}$	u	b	a
cL_2	u	a	b	$\overline{cL_2}$	u	b	a
cL_3	u	a	b	$\overline{cL_3}$	d	a	b
cR_1	d	a	b	$\overline{cR_1}$	u	a	b
cR_2	d	a	b	$\overline{cR_2}$	d	b	a
cR_3	u	b	a	$\overline{cR_3}$	d	b	a

$\overline{cR_2} \cap \overline{cR_3} = \overline{v_R}$, $\overline{cL_2} \cap \overline{cL_1} = \overline{v_L}$, $\overline{cR_3} \cap \overline{cL_1} = \overline{l_1}$ and $\overline{cR_1} \cap \overline{cL_3} = \overline{l_2}$. Then below $\overline{B_R}$ and above $\overline{B_L}$ is $\overline{lcP} = \overline{cR_2} \cup \overline{cR_3} \cup \overline{cL_1} \cup \overline{cL_2}$ a connection chain. Further, $\overline{ucP} = \overline{cL_3} \cup \overline{cR_1}$ is a connected chain above $\overline{B_R}$ and below $\overline{B_L}$. In fact, \overline{lcP} is the lower and \overline{ucP} the upper chain of the hstar \overline{CP} whose asymptotes are $\overline{B_R}, \overline{B_L}$. What's more, the respective chains have vertical bounding supporting lines at the points $\overline{l_i}$, $i=1, 2$, a supporting line at $\overline{l_i}$ is unique when the asymptote l_i joins (the same) ideal endpoints. Finally, since $\overline{l_1} \neq \overline{l_2}$, \exists a vertical line \overline{V} with $x(\overline{l_1}) < x(\overline{V}) < x(\overline{l_2})$ so \overline{CP} in the claimed hstar. All arguments in the proof are valid in the opposite direction so the converse is also true. As 2(b) this case is also self-dual. q.e.d.

Estars, pstars and hstars can be considered as estars whose boundary has none, one, or two ideal points respectively.⁹ This can be seen from the first part of each Fig. 15 through Fig. 20 by viewing the original gconic on the model of the projective plane where estars contain no diameters of the capping disk, pstars have one diameter and hstars two. In the case of hstars the diameters on the cap correspond to the hstar's asymptotes, while for a pstar the single diameter shows the direction where it meets l_∞ . In short, gconics are estars either away from, or touching or crossing l_∞ . The theorems message is that in parallel coordinates the image of a gconic is another gconic whose type can be determined by "inspection". Specifically, for a given gconic \overline{GC} find if \exists a line with slope $m=1$ intersecting only one of its components. If there is no such line then $\partial(\overline{GC})$ can not contain an ideal point $\Rightarrow \overline{GC}$ is an estar (case 3(a)). Otherwise, determine the maximum number of points $\partial(\overline{GC})$ can intersect a line with slope $m=1$. That number is either 1 or 2. If it is 1 then \overline{GC} is a pstar since the boundary contains one ideal point (cases 2(a) and (3(b)), and if 2 then \overline{GC} is an hstar (cases 1, 2(b) and 3(c)).¹⁰

The analogue of this theorem for conic sections was proved by Dimsdale using an algebraic argument [11]. In our case a direct synthetic

proof yielded the more general result. Incidentally, this Theorem includes the results in [16] which correspond to Cases 1 and 3(a). Recall our definition of gconics in terms of sections of a double cone whose base is an estar.¹¹ In light of the theorem it is natural to ask whether for an estar \overline{GC} the hstar \overline{GC} is a section of the same cone? This turned to be a surprisingly difficult problem and Dimsdale obtained an affirmative partial result again for ellipses and hyperbolas [12].

Corollary 1. (*Interior points of estars \leftrightarrow Interior lines to hstars.*) P is an interior point of an estar $\overline{CP} \Leftrightarrow \overline{P}$ separates \overline{LcP} and \overline{UcP} . (see Fig. 22).

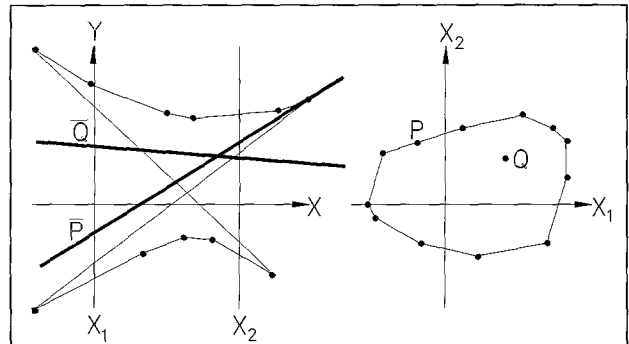


Fig. 22. Interior and boundary points of an estar (bounded convex set)

Corollary 2. (*Dual of Corollary 1. Interior lines to hstars \leftrightarrow Interior points of estars.*) If \overline{CP} is an hstar and \overline{CP} is an estar, then \overline{l} is an interior point of an estar $\overline{CP} \Leftrightarrow l$ separates LcP and UcP (the upper and lower chains of \overline{CP}).

There is a very useful property for the construction of the Convex-Hull. In parallel coordinates, the "outermost" portion of the envelope (of the family of straight lines representing the points of a set) is the *convex-hull of the set*. This is illustrated in Fig. 23 where the points $\overline{AB}, \overline{BC}, \overline{DE}, \overline{EF}$ representing the edges AB, BC, DE, EF of the set not in convex-hull are *inbetween* the envelope – formed by the extreme points – representing the convex-hull. It is stated below and exploited in [17].

⁹ We consider estars and pstars as having one component (i.e. consisting of one connected part in the Euclidean Plane), while hstars have two components

¹⁰ To complete the discussion, an estar which is completely above or below its waist (i.e. the waist is on the estar's boundary), is the dual of a dstar

¹¹ It is, of course, known that a convex set in R^N can be considered as a section of a convex cone in R^{N+1} (see [22] p. 15)

Corollary 3. (Convex-Hull of Bounded Sets.) Let BS be a bounded set and CBS its Convex-Hull.

Then

1. γ is an arc of $\partial(BS) \Leftrightarrow \bar{\gamma} \in \overline{CBS}$ or $\bar{\gamma}$ is below $uCBS$ and above $lCBS$ and,
2. $P \in \partial(CBS) \Leftrightarrow \exists$ a segment of the x -axis where $P \in \partial(BS)$ is above or below all other edges of $\partial(BS)$.

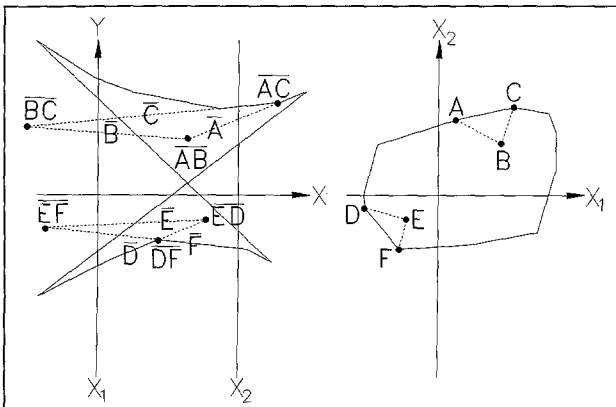


Fig. 23. Convex-Hull construction

That is, $\partial(\overline{CBS})$ consists of the highest and lowest portions of $\partial(BS)$. There is also an interesting “De-Morgan-like” duality between the operations of *Intersections* and *Convex Unions* of estars and their corresponding hstars. In the last section we provide a preview of this generalization to convex hypersurfaces in R^N .

The following remark is made in order to appreciate the results given in the next section. For the matrix A of our correlation $A^2 \neq A$ and therefore, our correlation is not a *polarity* (for a definition see [10] p. 60) and *our duality applied to convex sets is fundamentally different than the standard duality of Convexity Theory* (for a definition see [14] p. 46).

Intersections and convex unions are duals

Outer intersections of hstars

We construct next the unbounded extensions of the upper, UcP , and lower, LcP chains of an hstar \overline{CP} , namely

$$\overline{UCP} = \{\bar{p} | \bar{p} \text{ on or above } \overline{UcP}, \bar{V}_l \text{ and } \bar{V}_u\}$$

$$\overline{LCP} = \{\bar{p} | \bar{p} \text{ on or below } \overline{LcP}, \bar{V}_l \text{ and } \bar{V}_u\}.$$

The unbounded regions \overline{UCP} , \overline{LCP} are called the *Upper & Lower Branches* respectively of the hstar \overline{CP} . In this section, unless otherwise stated, \overline{CP} is considered as consisting of the two asymptotes and the two *branches*, rather than the customary two *chains*.

Next we define and study two operations on hstars, which yield an hstar. Roughly speaking the *Outer Intersection* of two hstars yields and hstar whose chains consist of the *outermost* portions of the two hstars. The *Inner Union*, on the other hand, is formed from the *innermost* chains of the two hstars.

The branches of an hstar are the set-theoretic complement of the region “inbetween” its chains and asymptotes.¹² We are now in a position to a “DeMorgan-like” duality between *Intersections of Estars with the Inner Union of the corresponding Hstars, and Convex Union of Estars with the Outer Intersection of their corresponding Hstars*. Here we consider the branches, that is the “complements” of their corresponding hstars.

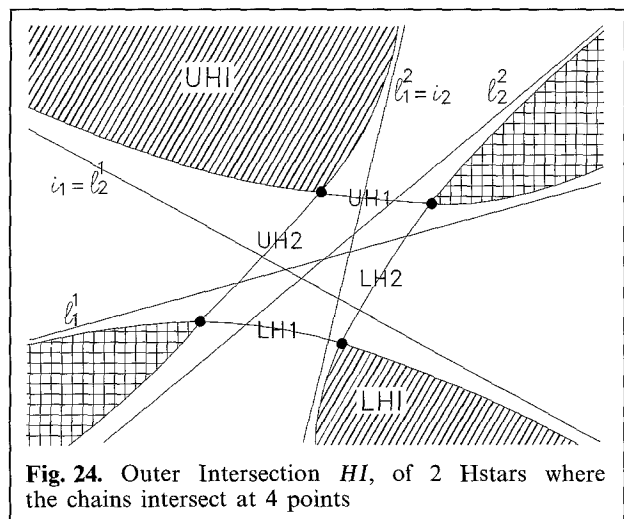


Fig. 24. Outer Intersection HI , of 2 Hstars where the chains intersect at 4 points

Definition (Outer Intersection of Hstars). Let $H1$ and $H2$ be two hstars, with respect to the ideal point having slope $\pm\infty$, having asymptotes l_i^1, l_i^2 , $i=1, 2$ respectively (for convenience we assume that $m(l_1^j) < m(l_2^j)$, $j=1, 2$ see Fig. 24).

¹² That is the region *below* the upper and *above* branches

Their *Outer Intersection*, $H1$, is the hstar whose asymptotes i_1, i_2 are the asymptotes with the minimum and maximum slope of the 2 hstars (i.e. $|m(i_1)| = \max \{|m(l_1^1)|, |m(l_1^2)|\}$ and $|m(i_2)| = \max \{|m(l_2^1)|, |m(l_2^2)|\}$), with and upper and lower branches defined respectively by

$$UHI = \{P \in H1 \cap H2 \text{ and above both } i_1, i_2\},$$

$$LHI = \{P \in H1 \cap H2 \text{ and below both } i_1, i_2\}.$$

By construction UHI, LHI is above, or below respectively *all four* asymptotes of the hstars. The hstar intersection *may or may not* be the set-theoretic intersection of the hstars. For example in Fig. 24 it is not and that occurs when the hstars are the images of *disjoint* estars (see Fig. 26 on p. 85). In either case we denote the intersection of the two hstars by $HI = H1 \cap H2$.

The intent of *Outer Intersection*, rather than *set-intersection*, will be explicitly mentioned if it is not clear from the context. The definition also applies to the intersection of hstars with respect to an ideal point having slope m resulting in an hstar with respect to the same ideal point. This is seen by first rotating the plane so that lines with slope m become vertical, intersecting the rotated hstars and then reversing the rotation back to the original orientation. The situation when the *outer intersection* coincides with the set-intersection of the hstars as shown in Fig. 25.

Theorem 2. If $E1$ and $E2$ are estars then $\overline{CU} = C[E1 \cup E2] = \overline{E1} \cap \overline{E2} = EI$.

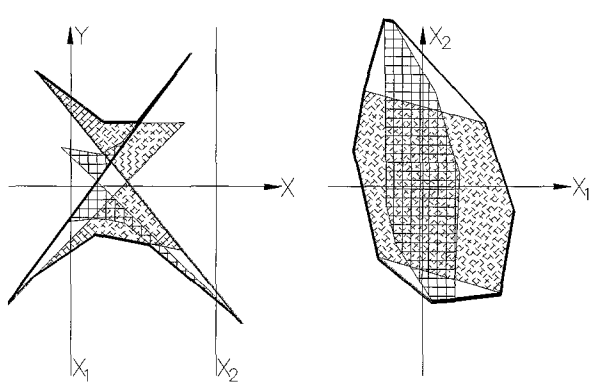


Fig. 25. Convex union of estars corresponds to the Outer intersection of their hstars

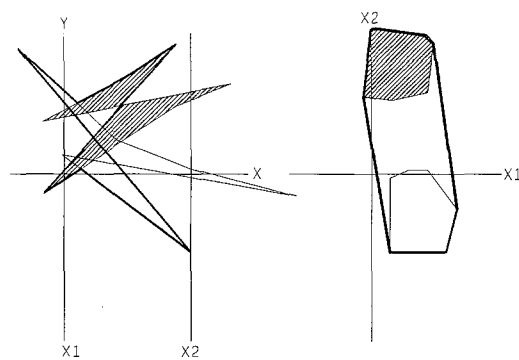


Fig. 26. Convex-Hull of disjoint estars

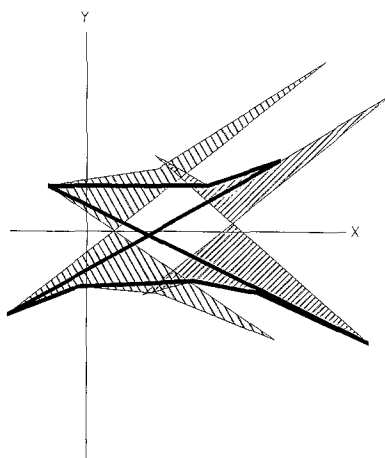


Fig. 27. The Convex Union of two Hstars as an Inner Union

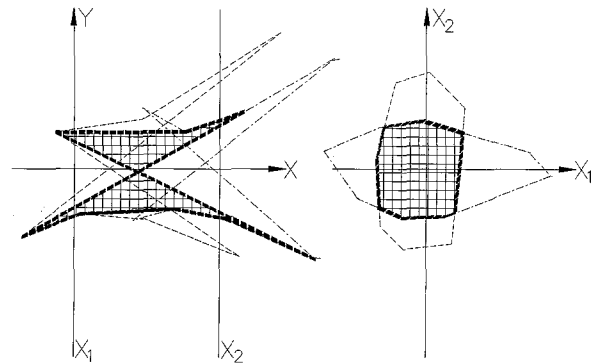


Fig. 28. Inner Union and Intersection are Dual

Proof. By definition \overline{EI} is the hstar whose boundary consists of the highest and lowest portions of $EI \cup E2$. By Corollary 2 then $C[EI \cup E2] = \overline{EI}$ and the theorem is proved.

Note again that the notation \overline{EI} can be considered as the complement of the hstar representing $E1$. Next by an easy induction we have that,

Theorem 3. (Convex union of a finite collection of estars.) If $ES_i, i=1, 2, \dots, n$ are estars then

$$\overline{C\left[\bigcup_{i=1}^{i=n} ES_i\right]} = \bigcap_{i=1}^{i=n} \overline{ES_i}$$

and the corresponding dual,

Theorem 4. (Outer intersection of a finite collection of hstars.) If $HS_i, i=1, 2, \dots, n$ are hstars with respect to the ideal point having slope 1 then

$$\overline{\bigcap_{i=1}^{i=n} HS_i} = C\left[\bigcup_{P_i=1}^{i=n} \overline{HS_i}\right].$$

Since the union of a countable collection of bounded sets may not be bounded, Theorem 3 is true in general only for finite collections. Also a countable collection of hstars may have in its intersection a vertical edge or asymptote so Theorem 4 is again only true in general for the intersection of finite collections of hstars.

Inner union of hstars

Definition (Inner union of hstars). Let $H1$ and $H2$ be two hstars, with respect to the ideal point having slope $\pm\infty$, u_1, u_2 the two supporting lines between $UHU' = C[UH1 \cup UH2]$ and $LHU' = C[LH1 \cup LH2]$ (i.e. the Convex Union of the Upper and Lower Branches), at the points $u_i \cap UHU' = U_i$ and $u_i \cap LHU' = L_i$ for $i = 1, 2$. Let uHU and lHU be the finite portions of $\partial(UHU')$ and $\partial(LHU')$ between the points U_i and L_i respectively. The hstar with asymptotes u_i and uHU, lHU as upper and lower chains is called the *Inner Union of the Hstars H1 and H2* (see Fig. 27).

The definition also applies to the inner union of hstars with respect to an ideal point having

slope m resulting in an hstar with respect to the same ideal point. This is seen by first rotating the plane so that lines with slope m become vertical, taking the inner union of the rotated hstars and then reversing the rotation back to the original orientation.

The significance of the supporting lines to the the upper and/or lower chains of $H1$ and $H2$, added as result of the Convex Union operation (see Fig. 27) will be seen after Theorem 5. Note also that the asymptotes of the Inner Union are in general different than those of either hstar.

Theorem 5. If $E1$ and $E2$ are estars then $E1 \cap E2 = C[\overline{E1} \cup \overline{E2}]$.

Proof. Is direct from Corollary 1. That is, $P \in E1 \cap E2 \Leftrightarrow \overline{P}$ separates the upper and lower chains of both $E1$ and $E2$. So P is in-between $UBE1 \cup UE2$ and $LE1 \cup LE2$ (here the set-theoretic union is meant). The intersection of the estars is an estar. Therefore, by part 2 of Corollary 3 the collection of all \overline{P} such that $P \in \partial(E1 \cap E2)$ forms the boundary of $C[\overline{E1} \cup \overline{E2}]$ q.e.d. (see Fig. 28).

The supporting lines added to the hstars by the Inner Union Operation correspond to the points of intersection between the boundaries of the corresponding estars. For consistency with the Outer Intersection operation we can consider points of tangency as double points. Inductively we can obtain the result for countably infinite families of estars.

Theorem 6. If $ES_i, i=1, 2, \dots$ are estars then

$$\overline{\bigcap_{i=1}^{i=\infty} ES_i} = C\left[\bigcup_{i=1}^{i=\infty} \overline{ES_i}\right],$$

whose dual is

Theorem 7. If $HS_i, i=1, 2, \dots$ are hstars with respect to the ideal line having slope 1 then

$$C\left[\bigcup_{i=1}^{i=\infty} HS_i\right] = \overline{\bigcap_{i=1}^{i=\infty} HS_i}.$$

By contrast to the previous section, here the theorems are true for countably infinite families of estars since the intersection of any family of estars is an estar. Theorems 3, 4, 6 and 7 are, of

course reminiscent of the similar relationship between convex sets and their *polar* sets (see [22] p. 150).

Special points

Some “special points” attract our attention when we look at a curve. What are the properties of such points in parallel coordinates? For an *LP*-curve¹³ γ let I_1 and I_2 denote its *projections (intervals)* on the x_1 and x_2 axes respectively. On I^1 let P_m, P_M denote the points where γ attains its *absolute minimum* and *absolute maximum* respectively. In parallel coordinates P_m, P_M are the *supporting lines to $\bar{\gamma}$* through the points $(1, \alpha_m)$ and $(1, \alpha_M)$ on the x_2 parallel axis, where $\alpha_m = \min\{\alpha \in I_2\}$ and $\alpha_M = \max\{\alpha \in I_2\}$. A point P_0 is a zero of $\gamma \Leftrightarrow P_0$ is a *supporting line to $\bar{\gamma}$ through the point $(1, 0)$ on the x_2 parallel axis*. Below as usual we denote the *chain* of the two convex *LP*-curves r_1, r_2 joined at the point N by r_1Nr_2 , and the slope of a line n by $m(n)$.

Let r_1, r_2 be two convex *LP*-curves joined at the point N , having a common tangent n there such that *locally*¹⁴ $\forall P_1 \in r_1, P_2 \in r_2$ the slopes $m(l_1) \neq m(l_2)$ where l_i is the supporting line to r_i at P_i . The point N is called a *cusp* of the chain r_1Nr_2 – see the right hand portion of Fig. 29. Further,

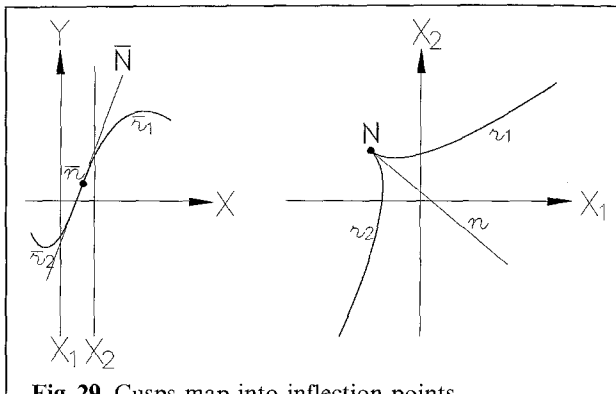


Fig. 29. Cusps map into inflection points

let r_1, r_2 be convex upward and convex downward *LP*-curves respectively joined at the point N and with a common supporting line n there and such that locally if $P_1 \in r_1$ and l_1 is the

¹³ Here, to avoid verbiage we use the terms *function* and the *curve or graph* of the function interchangeably

¹⁴ By this we mean that there \exists a neighborhood of the point N where the stated property is true

supporting line to r_1 at P_1 , $\exists P_2 \in r_2$ with l_2 the supporting line to r_2 at P_2 and $m(l_1) = m(l_2)$. The point N is called an *inflection point* of the chain r_1Nr_2 – see the right hand portion of Fig. 30.

The tangent n to an *LP*-chain at either a cusp or inflection point *crosses* the chain at that point in the sense that part of the chain is above and part below the line n . Hence, the chain is not convex. There is a striking and potentially very useful duality between these two kinds of “nonconvex” points.

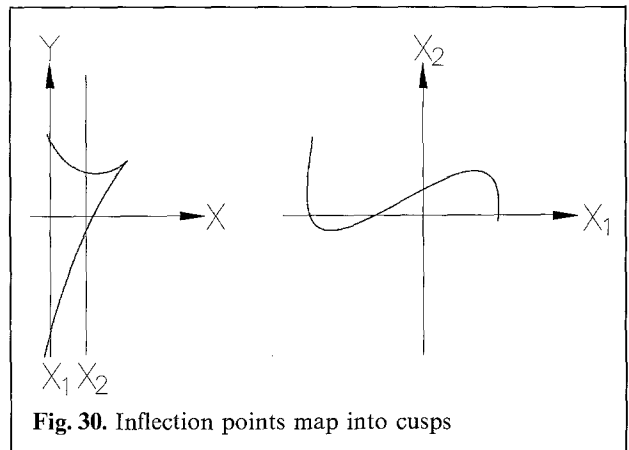


Fig. 30. Inflection points map into cusps

Theorem 8. For $m(n) \neq 1$, r_1Nr_2 has a cusp with tangent n at $\bar{N} \Leftrightarrow r_1Nr_2$ has an inflection point with tangent \bar{n} at \bar{n} .

Proof. Let r_1, r_2 be two convex *LP*-curves joined in a *cusp* at the point N with a common tangent n there having slope $m(n)$ as shown in Fig. 29. Assume further that $m(n) < 1$. Then, locally r_1 is above n with $1 > M_1 \geq m(n)$ ¹⁵, and r_2 is below n with $M_2 \leq m(n)$. Since n is a supporting line to both r_1 and r_2 at N then r_1 must be convex upward and r_2 convex downward. Hence, by Lemma 4a \bar{r}_1 is convex downward and \bar{r}_2 is convex upward, and Lemma 3a \Rightarrow they lie on *opposite* sides of their common tangent \bar{n} at \bar{n} . This means that r_1Nr_2 has either a cusp or an inflection point at \bar{n} . If it has a cusp then \exists a point $\bar{l}_1 \in \bar{r}_1$ and another point $\bar{l}_2 \in \bar{r}_2$ with $x(\bar{l}_1) = x(\bar{l}_2) \Rightarrow l_1$ is a supporting line of r_1 and l_2 is a supporting line of r_2 and by (2)¹⁶

¹⁵ Again, M_i denotes the maximum slope of the supporting lines to r_i on the interval of x_1 in question

¹⁶ See also Figs. 3 and 7

they must have the same slope. This is impossible since $M_1 \geq m(n) \geq M_2$. Hence, $r_1 N r_2$ has an inflection point at n .

For $m(n) > 1$, r_1 convex downward and r_2 convex upward, Lemma 4b $\Rightarrow r_1 \dots$ is convex upward and r_2 is convex downward. The proof is then the same as above with the roles of r_1 and r_2 interchanged.

Finally when $m(n) = 1$, locally $M_i \leq 1$ and $M_2 \leq 1$. Lemma 4 \Rightarrow that both r_1 and r_2 are convex downward when r_1 is convex downward, or both convex upward when r_1 is convex upward. In either case, Lemma 3 \Rightarrow both r_1, r_2 are on the same side of \bar{N} joined at the ideal point \bar{n} .

To prove the converse, let \bar{r}_1, \bar{r}_2 be convex downward and convex upward LP-curves respectively joined at the inflection point \bar{n} , with \bar{r}_1 below and \bar{r}_2 above their common supporting line N there. Therefore, \bar{r}_1 is above and \bar{r}_2 below the point \bar{n} . Assume at first that $x(\bar{n}) \geq 0 \Rightarrow m(n) < 1$. So locally $M_i < 1$ for $i = 1, 2 \Rightarrow r_1, r_2$ are convex upward and convex downward respectively. Since $r_1 N r_2$ has an inflection point at \bar{n} , locally the slope of the supporting lines P_1 at $\bar{l}_1 \in \bar{r}_1$ increases monotonically to $m(\bar{N})$. Similarly, the slope of the supporting lines, P_2 of \bar{r}_2 decreases monotonically to $m(\bar{N})$. This means that in a neighborhood of $\bar{n} \forall P_1 \exists P_2$ with $m(P_1) = m(P_2) \Rightarrow$ in a neighborhood of $N \forall P_1 \# r_1 \exists P_2 \in r_2$ such that $x_1(P_1) = x_1(P_2)$ ¹⁷. We have proved that $r_1 N r_2$ has a cusp at N with common tangent n .

When $x(\bar{n}) \leq 0$ then $m(n) > 1$ and the proof is the same with the roles of r_1 and r_2 being reversed. The case $m(n) = 1$ is easily recognized since then both \bar{r}_1, \bar{r}_2 are on the same side of \bar{N} , joined at the ideal point \bar{n} , and both are either convex upward or convex downward. q.e.d.

Theorem 9. For $m(n) \neq 1$, $r_1 N r_2$ has an inflection point with tangent n at $\bar{N} \Leftrightarrow r_1 N r_2$ has a cusp with tangent \bar{N} at \bar{n} .

Proof. The proof is obtained by interchanging the roles of r_i with \bar{r}_i for $i = 1, 2$ in the proof of the previous theorem – see also Fig. 30.

¹⁷ This is a consequence of the correlation $C_B: P \leftarrow \rightarrow \bar{P}$ (see p. 3) corresponding to the property of parallel lines in the correlation $C_A: l \leftarrow \rightarrow \bar{l}$

Some applications

In [17], some algorithms based on these results are described. They include an algorithm for convex-hull construction which is optimal in the sense of [4]. It is $O(n \log n)$ for worst-case and $O(n \log n)$ for real-time construction, as well as $O(n)$ expected time (for certain distributions of the data). Also included are algorithms for the intersection of families of half-planes and collections of convex sets. Other early applications include Modility Analysis in Robotics [9] and Dynamical Systems [21]. Potentially, we believe, that some of the included results will find significant applications in VLSI design (e.g. intersection of large collections of convex sets, finding interior points to hypersurfaces – see next section), Computer Graphics and CAD (e.g. fast rotations – see next section, Solid Body Modeling), Pattern Recognition (e.g. using the cusp $\leftarrow \rightarrow$ inflection point and the point $\leftarrow \rightarrow$ line dualities) and others.

In the remainder we provide a synopsis of some corresponding results in R^N . This is done both as a “preview” and in order to provide credibility to the claim that parallel coordinates are suitable for Multi-Dimensional Graphics.

Results for R^N

Lines in R^N

Our objective is to represent multivariate relations geometrically. A line l in N -space is the collection of points $(c_1, c_2, \dots, c_i, \dots, c_N)$ satisfying the linear relations:

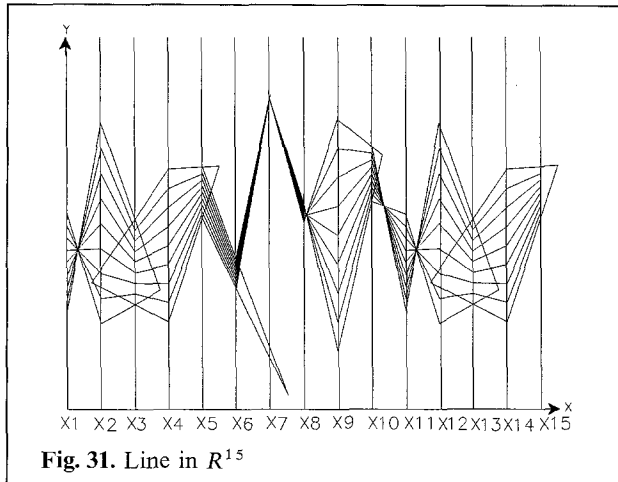
$$\begin{aligned} l_{12}: \quad & x_2 = m_2 x_1 + b_2 \dots \\ l_{1i}: \quad & x_i = m_i x_1 + b_i \dots \\ l_{1N}: \quad & x_N = m_N x_1 + b_N. \end{aligned} \tag{6}$$

for $i = 2, \dots, N$. In the $x_1 x_i$ -plane the relation labeled l_{1i} is a line. By (2), in parallel coordinates \bar{l}_{1i} is a point. There are $N - 1$ such independent relations in (6). Therefore, the line l is represented by the $N - 1$ points \bar{l}_{1i} for $i = 2, 3, \dots, N$. One variable, x_1 , was chosen in (6) as the parameter. It is sometimes convenient to describe a line l in R^N by linear equations relating consecutive variables. Specifically:

$$l_{i,i+1}: \quad x_{i+1} = m_i x_i + b_i. \tag{7}$$

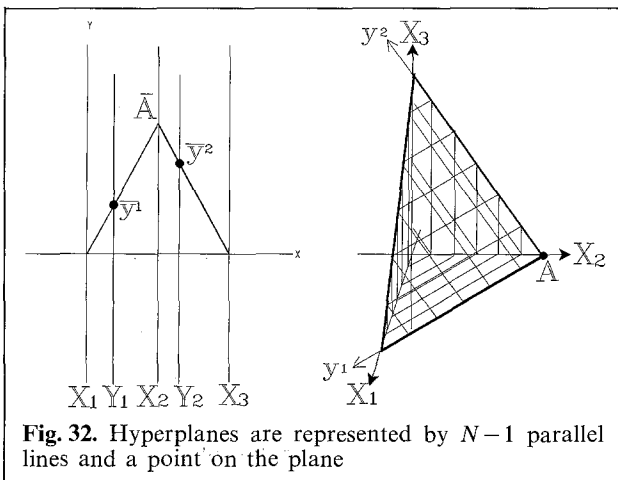
for $i = 2, \dots, N$.

In Fig. 31 we see points on a line in R^{15} described by a set of 14 equations of type (7). These polygonal lines show us particular set of *linearly dependent vectors*. For $N > 2$ intersection of lines is very rare but it may happen. Such intersections can be “seen” in parallel coordinates and they resemble “particle collisions” (see [15] p. 37).



Hyperplanes

Consider a plane Π in R^3 as shown in Fig. 32 and the two lines $Y^1 = \Pi \cap x_1 x_2$ -plane, $Y^2 = \Pi \cap x_2 x_3$ -plane. We can construct a coordinate system on Π with axis Y^i $i=1, 2$ and $A = Y^1 \cap Y^2$ as origin. Therefore, every point of Π can be specified as the intersection of two



unique lines, parallel to Y^1 and to Y^2 respectively. Or, equivalently, from the collection of all lines parallel to Y^1 and Y^2 we can specify all points in the plane.

The purpose of this discussion is to show that a plane Π can be equivalently specified in terms of two families of parallel lines. So in parallel coordinates a plane is represented by two vertical lines, say Y_1 and Y_2 corresponding to the lines parallel to Y^1 and Y^2 respectively. But we are not quite finished. All planes parallel to Π can be specified by a coordinate system parallel to the Y^1 and Y^2 axis. To identify a specific such plane we need in addition a point on the plane. We pick A the origin of the coordinate system.

Just as for lines this reasoning generalizes to N -space. There a $N-1$ parallel lines and a polygonal line (representing a point) represent a hyperplane. Specifically, for a hyperplane Π & construct hyperplane is represented the $N-1$ lines $Y^i = \Pi \cap x_i x_{i+1}$ -plane for $i=1, \dots, N-1$. Proceeding, we have $N-1$ collections of parallel lines to the Y^i and which are manifested as $N-1$ vertical lines in parallel coordinates. Choosing in addition a specific point on Π completes the representation. In parallel coordinates hyperplanes can be intersect with lines or with other hyperplanes. The later construction enables us graphically to solve systems of N linear equations in N variables, and also to study error propagation graphically!

Perhaps the most striking geometrical aspect of the hyperplanes representation is, as in 2-D, that in 3-D the rotation of a plane about a line is converted into a translation of a point a line. The reader interested in a in-depth treatment of lines and hyperplanes using parallel coordinates is referred to [15].

Convexity in R^N

The easiest hypersurfaces to show are those with a high degree of symmetry. In Fig. 33(a) we see a square with unit side in orthogonal and parallel coordinates; note that the coordinates of the vertices are ordered couples of 0's and 1's. In Fig. 33(b) we see that the “unit” cube in R^3 , i.e. whose vertices have ordered triples of 0's and 1's as coordinates, is represented in parallel coordinates by two copies of

the unit square. The edges and faces of the cube can also be found from its representation in parallel coordinates. In R^N , $N-1$ copies of the square represent the “unit” hypercube. The comparable hypercube in R^5 is shown in Fig. 33(c).

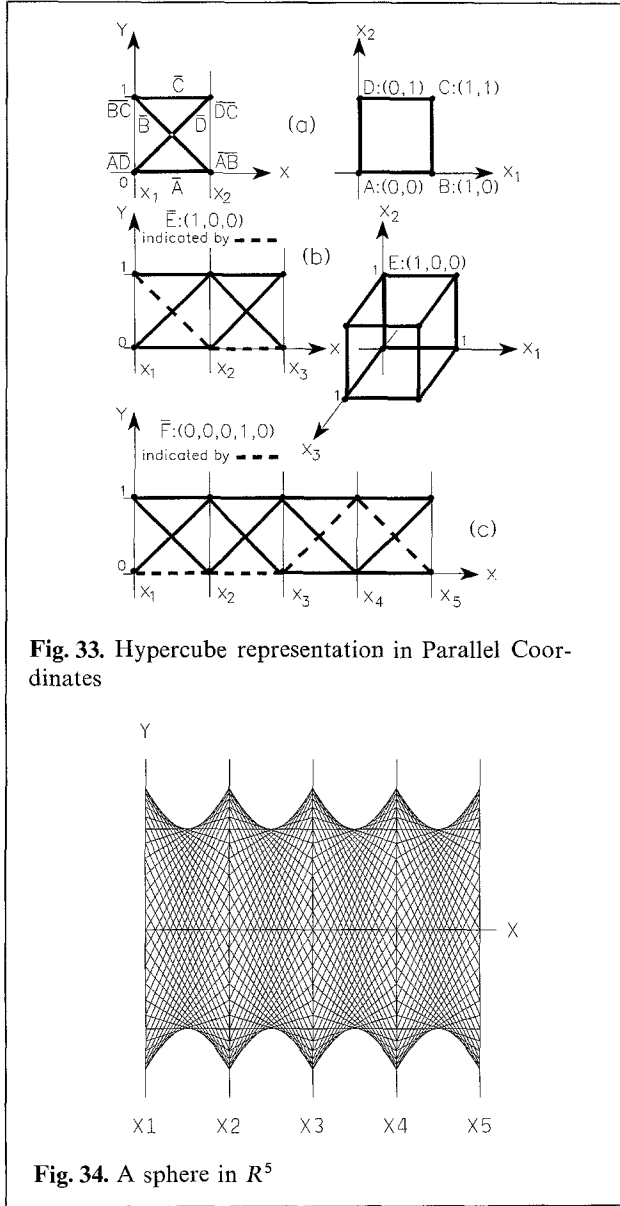


Fig. 33. Hypercube representation in Parallel Coordinates

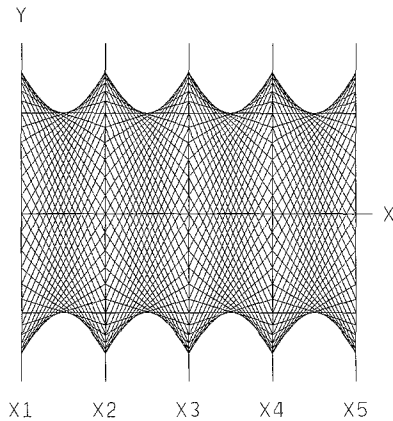


Fig. 34. A sphere in R^5

This “symmetry principle” is completely general. For example, in Fig. 34 is the representation of a sphere in R^5 . Recall (see also Fig. 15) that an ellipse is represented by a hyperbola (i.e. $\text{estar} \leftrightarrow \text{hstar}$). This is a sphere centered at the

origin and with radius r . Between the parallel axis we see the same hyperbola which, in turn, represents a circle with radius r . So a hypersphere in R^N centered at the origin is represented by $N-1$ copies of a circle – having the same radius as the sphere – and also centered

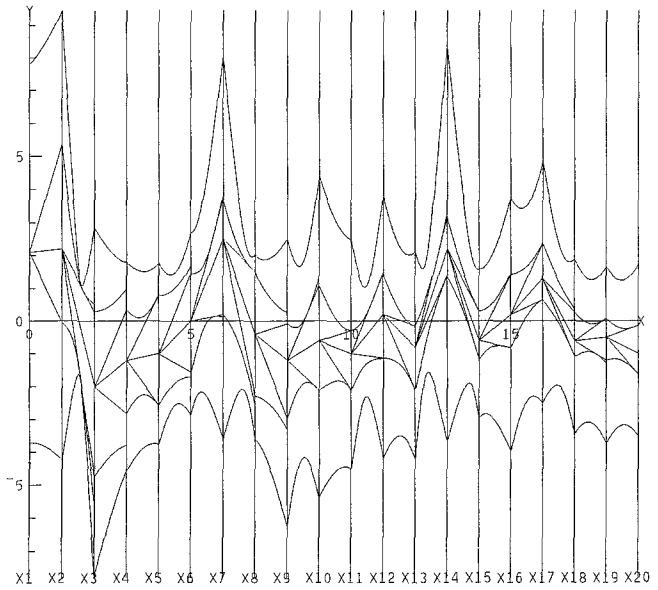


Fig. 35. Finding a point interior to a hypersurface in R^{20}

at the origin. For more general convex hypersurfaces, we can obtain their parallel coordinate representation by computing the *envelope* of the collection of polygonal lines representing its points – i.e. by going to the the basic and general definition given at the beginning. In Fig. 35 we show the representation of a convex hypersurface in R^{20} ! This “picture” reveals a lot of information about the hypersurface. In particular, there is an algorithm which enables us to find whether a *given point is inside, outside, or on the surface*. A polygonal line which was found to represent an interior point of the hypersurface is shown in the figure. This algorithm has exciting implications. A process (like in a industrial plant, or a function of biological organism, the motion of a robot) is a relation among many variables. Such a relation corresponds to a particular hypersurface which we may able to represent in parallel coordinates. *Controlling the process corresponds to staying in the INTERIOR of the hypersurface. Intelligent Process Control and Intelligent CAI based on this algorithm are presently being explored.*

Acknowledgement. It is a pleasure to acknowledge the valuable suggestions and help received from B. Dimsdale, A. Hurwitz, T. Chomut, M. Mostrel, G. Sassouni and L. Yashar. Multi-Dimensional Graphics has been partially implemented using VS APL GRAPHPAK which together with IPG and GRACOL were used for the graphics shown here. The paper was composed on an ICEF and printed by APA 6670. All acronyms refer to IBM product offerings.

References

1. Ayres F (1967) Projective geometry. Schaum's Outline Series In Mathematics, McGraw-Hill, New York
2. Banchoff TF, Strauss CM (1979) Real time computer graphics analysis of figures in four-space in [5] pp. 159-167
3. Barnett V Edit. (1981) Interpreting multivariate data. Wiley, New York
4. Bentley JL, Shamos MI (1978) Divide & conquer for linear expected time. Infor Proc Letters 7:87-97
5. Brissom D (ed.) (1979) Hypergraphics: visualizing complex relationships in art, science and technology. Am Assoc Adv Sci. Westview Press, Boulder
6. Brodetsky OS (1949) A first course in nomography. G. Bell & Sons, London (First Published 1920)
7. Burton RP, Smith DR (1982) A hidden-line algorithm for hyperspace. SIAM J. Comput. 11:71-80
8. Busemann H, Kelly PJ (1953) Projective geometry and projective metrics. Academic Press, N.Y.
9. Cohan S (1984) Mobility analysis using parallel coordinate (to appear) in J Inter Fed Theory Mach Mech Available as IBM Los Angeles Scientific Center Report # G320-2754
10. Coxeter HSM (1974) Projective geometry. Univ. of Toronto Press, Toronto
11. Dimsdale B (1981) Conic transformations. IBM Los Angeles Scientific Center Report # G320-2713, October
12. Dimsdale B (1984) Conic transformations & projectivities. IBM Los Angeles Scientific Center Report # G320-2753
13. Hilbert D, Cohn-Vossen S (1952) Geometry and the imagination. Chelsea, New York
14. Grunbaum B (1967) Convex polytopes. Wiley, New York
15. Inselberg A (1981) N-dimensional graphics. Part I: Lines & hyperplanes. IBM Los Angeles Scientific Center Report G320-2711
16. Inselberg A, Reif M (1984) Convexity in parallel coordinates, submitted for publication. Presently available as IBM Los Angeles Scientific Center Report # G320-2738
17. Inselberg A, Reif M, Chomut T (1985) Convexity algorithms in parallel coordinates (to be submitted for publication)
18. Isaacson PL, Burton RP, Douglas DM (1984) Presentation of hypothesized 4-D phenomena. Comput Graph World 48-63
19. Osgood WF (1925) Advanced calculus. Macmillan, New York, pp. 186-194
20. Mersereau MR, Oppenheim AV (1974) Digital reconstruction of multidimensional signals from their projections. Proc IEEE 62:1319-1337
21. Rivero J, Inselberg A (1984) Extension al analisis del Espacio De Fase de Systemas Dinamicos por las Coordenadas Paralelas. Proc VII Systems Engr Workshop. Santiago Chile July 1984
22. Rockafellar RT (1970) Convex analysis. Princeton University Press, Princeton